Available online at www.sciencedirect.com
SCIENCE DIRECT®
Fluid Phase Equilibria 224 (2004) 285–304
FLUID PHASE EQUILIBRIA
www.elsevier.com/locate/fluid

VLE predictions with the Peng–Robinson equation of state and temperature dependent k_{ij} calculated through a group contribution method

Jean-Noël Jaubert*, Fabrice Mutelet

Laboratoire de Thermodynamique des Milieux Polyphasés, Institut National Polytechnique de Lorraine, Ecole Nationale Supérieure des Industries Chimiques, 1 rue Grandville, 54000 Nancy, France

Received 24 January 2004; accepted 25 June 2004

Abstract

A group contribution method allowing the estimation of the temperature dependent binary interaction parameters ($k_{ij}(T)$) for the widely used Peng–Robinson equation of state (EOS) is proposed. A key point in our approach is that the k_{ij} between two components i and j is a function of temperature (T) and of the pure components critical temperatures (T_{Ci} and T_{Cj}), critical pressures (P_{Ci}, P_{Cj}) and acentric factors (ω_i, ω_j). This means that no additional properties besides those required by the EOS itself (T_C, P_C, ω) are required. Because our model relies on the Peng–Robinson EOS as published by Peng and Robinson in 1978 and because the addition of a group contribution method to estimate the k_{ij} makes it predictive, we decided to call this new model PPR78 (predictive 1978, Peng–Robinson EOS).

In this paper six groups are defined: CH_3, CH_2, CH, C, CH_4 (methane), and C_2H_6 (ethane) which means that it is possible to estimate the k_{ij} for any mixture of saturated hydrocarbons (*n*-alkanes and branched alkanes), whatever the temperature.

The results obtained in this study are in many cases very accurate and often better than those obtained with the best EOS/g^E models. In particular, it is shown that asymmetric systems can be accurately predicted with our model. Some comparisons are given with the LCVM model.

Keywords: Equation of state; Vapor–liquid equilibrium; Predictive model; Binary interaction parameters; Asymmetric mixtures

1. Introduction

Today, modern process design requires models capable of (i) predicting the equilibrium properties without the preliminary use of experimental data; (ii) yielding accurate results in both the sub-critical and critical regions. Simultaneous fulfillment of these requirements is a very difficult and challenging task for EOS. In order to meet these requirements, over the past 25 years, the classical van der Waals mixing rules with k_{ij} lost interest for many laboratories of thermodynamics worldwide and a new class of mixing rules has been proposed for the description of VLE using cubic EOS. All these methods, called EOS/g^E models, are based on equating the excess Gibbs energy from a liquid phase activity coefficient model with the corresponding term from an EOS. More information and comparison between all these methods can be found elsewhere [1–18]. Among these many EOS/g^E models, one was developed by Péneloux and co-workers [16–18]. In contrast to many other models, Péneloux did not use UNIFAC as the g^E model, but instead a Van Laar expression (see Eq. (1)):

$$g^E = \frac{1}{2}\frac{\sum_{i=1}^{N}\sum_{j=1}^{N} x_i x_j b_i b_j E_{ij}(T)}{\sum_{i=1}^{N} x_i b_i}$$

$$\text{with } \begin{cases} E_{ij} = E_{ji} \\ E_{ii} = 0 \end{cases} \quad \text{and} \quad \begin{cases} x_i = \text{mole fraction} \\ b_i = \text{covolume} \\ N = \text{number of components} \end{cases} \tag{1}$$

* Corresponding author. Fax: +33 3 83 17 51 52.
E-mail address: jean-noel.jaubert@ensic.inpl-nancy.fr (J.-N. Jaubert).

0378-3812/$ – see front matter © 2004 Elsevier B.V. All rights reserved.
doi:10.1016/j.fluid.2004.06.059

In order to obtain a predictive model, Péneloux developed, following the previous work of Kehiaian et al. [19], a group contribution method (GCM) to estimate the interaction parameter $E_{ij}(T)$ in Eq. (1). By doing so, Péneloux et al. were able to obtain a fascinating result: indeed, they showed that the combination at constant packing fraction of a cubic EOS and a Van Laar type g^E model was strictly equivalent to use classical mixing rules (linear on b and quadratic on a) with temperature dependent k_{ij}. In other words, for the first time, Péneloux et al. found a theoretical expression for the binary interaction parameters k_{ij}. Indeed, they established a simple relation between E_{ij} of the Van Laar model and k_{ij}. Such a result is very important because it is well-known that it is extremely difficult to correlate k_{ij} with respect to either substance types or temperature. From our point of view, the work by Péneloux et al. has one enormous advantage: it builds a bridge between the classical mixing rules (with k_{ij}) and the EOS/g^E models.

Even though accurate, Péneloux's model [17,18] has some disadvantages. Indeed, these authors did not use the original Peng–Robinson EOS but instead a "translated PR type EOS" in which the classical molar volume (v) and covolume (b) are replaced by the same translated quantities noted as $\tilde{v}$ and $\tilde{b}$ (the connection between $\tilde{v}$, $\tilde{b}$, v and b is not so easy to establish). Moreover, in order to estimate the attractive parameter $a(T)$ of their EOS, they defined two classes of pure compounds. For components which are likely to be encountered at very low pressure, the Carrier–Rogalski–Péneloux (CRP) $a(T)$ correlation [20] which requires the knowledge of the normal boiling point was used. For other compounds, they used a Soave-like expression [21] which is different from the one developed by Soave for the SRK EOS and different from the one developed by Peng and Robinson for their own equation. Moreover, to estimate E_{ij} (Eq. (1)), the decomposition into groups of the molecules is not straightforward and is sometimes difficult to understand. For example, propane is classically decomposed into two CH_3 groups and one CH_2 group but 2-methyl propane $\{CH_3{-}CH(CH_3){-}CH_3\}$ is decomposed into four CH groups and not into three CH_3 groups and one CH group. Isopentane is formed by one CH_3 group, half a CH_2 group and three-and-a-half CH groups. Lastly, because this model was developed 15 years ago, the experimental database they used to fit their parameters is small in comparison to what could be obtained today. The group parameters obtained from this too small database may lead to unrealistic phase equilibrium calculations at low or at high temperatures. For all these reasons, this very good theoretical model was never used by other research groups (except may be a few French groups) and never appeared in commercial process simulators.

The aim of this work is to develop a GCM allowing us to estimate the k_{ij} for the widely used PR EOS. To express k_{ij} in terms of group contributions, we only use equations coming from the past work of Péneloux et al. [18]. That is simple because Péneloux et al. expressed E_{ij} (Eq. (1)) in terms of group contributions but they also established a mathematical relation between $E_{ij}(T)$ and $k_{ij}(T)$. This mathematical relation also involves some properties of pure components i and j and some characteristics of the considered cubic EOS. This means that, in this study, the k_{ij} are temperature dependent. In this paper six groups are defined: CH_3, CH_2, CH, C, CH_4 (methane), and C_2H_6 (ethane) which means that it is possible to estimate the k_{ij} for any mixture of saturated hydrocarbons (n-alkanes and branched alkanes), whatever the temperature. We are planning to add many new groups soon (CO_2, N_2, H_2S, groups for aromatic and naphthenic hydrocarbons). A key point in our approach is that the k_{ij} between two components i and j is a function of temperature (T), of the critical temperatures (T_{Ci} and T_{Cj}), of the critical pressures (P_{Ci}, P_{Cj}) and of the acentric factors (ω_i, ω_j). This means that no additional properties (e.g. the critical volume) besides those required by the EOS itself (T_C, P_C, ω) are required. Because our model relies on the Peng–Robinson EOS as published by Peng and Robinson in 1978 [22] and because the addition of a GCM to estimate the k_{ij} makes it predictive, we have decided to call this new model PPR78 (predictive 1978, Peng–Robinson EOS).

The results obtained in this study are in many cases very accurate and often better than those obtained with the best EOS/g^E models. In particular, it is shown that asymmetric systems are accurately predicted with our model. Some comparisons are made with the LCVM model (the best one for this kind of system). This paper thus gives proof that the van der Waals one-fluid (vdW1f) mixing rules can be used for asymmetric systems. Indeed, despite the results obtained by Harismiadis et al. [23], Coutinho et al. [24] and Gao et al. [25], many investigators still believe that the vdW1f mixing rules do not apply to this kind of system. For example, Gao et al. [25], by using the PR EOS and temperature dependent k_{ij} were able to correlate 1500 bubble-point pressures of different binary systems (containing alkanes up to n-C_{44}) with an average overall deviation of 2.3%.

To conclude, let us stress that this work has been conducted because in the open literature, many correlations to estimate the k_{ij} can be found. However, all these correlations only apply to specific mixtures (e.g. mixtures containing hydrocarbons and methane [26], mixtures containing hydrocarbons and nitrogen [27], mixtures containing hydrocarbons and carbon dioxide [28], mixtures containing light hydrocarbons [29], etc.). In fact, there are so many of them that it is impossible to detail all the references here. Moreover, most of the proposed correlations are purely empirical and often unsuitable for extrapolation. Finally, these correlations often use additional properties besides those (the critical properties and the acentric factor) required by the cubic EOS. By using, as illustrated in this paper, a group contribution method with a theoretical basis, we avoid all these drawbacks.

2. The PPR78 model

2.1. The equation of state

In 1976, Peng and Robinson [30] published their well-known equation of state, called in this paper PR76. In 1978, Peng and Robinson [22] published an improved version of their equation of state, which yields more accurate vapor pressure predictions for the heavy hydrocarbons than those obtained by using PR76. This improved equation is called PR78 in this paper. For a pure component, the PR78 EOS is

$$P = \frac{RT}{v - b_i} - \frac{a_i(T)}{v(v + b_i) + b_i(v - b_i)} \tag{2}$$

with

$$\begin{cases} R = 8.314472\,\mathrm{J\cdot mol^{-1}\cdot K^{-1}} \\ b_i = 0.0777960739\frac{RT_{\mathrm{C},i}}{P_{\mathrm{C},i}} \\ a_i = 0.457235529\frac{R^2T_{\mathrm{C},i}^2}{P_{\mathrm{C},i}}\left[1 + m_i\left(1 - \sqrt{\frac{T}{T_{\mathrm{C},i}}}\right)\right]^2 \\ \text{if } \omega_i \le 0.491\ldots m_i = 0.37464 + 1.54226\omega_i - 0.26992\omega_i^2 \\ \text{if } \omega_i > 0.491\ldots m_i = 0.379642 + 1.48503\omega_i \\ \qquad\qquad - 0.164423\omega_i^2 + 0.016666\omega_i^3 \end{cases} \tag{3}$$

where P is the pressure, R the ideal gas constant, T the temperature, a and b are EOS parameters, v the molar volume, T_{C} the critical temperature, P_{C} the critical pressure and ω the acentric factor.

In this paper, the PR78 EOS is used. To apply such an EOS to mixtures, mixing rules are used to calculate the values of a and b of the mixtures. Classical mixing rules are used in this study:

$$a = \sum_{i=1}^{N}\sum_{j=1}^{N} z_i z_j \sqrt{a_i a_j}(1 - k_{ij}(T)), \qquad b = \sum_{i=1}^{N} z_i b_i \tag{4}$$

where z_k represents the mole fraction of component k in a mixture, and N the number of components in the mixture. In Eq. (4), the summations are over all chemical species. $k_{ij}(T)$, whose choice is difficult even for the simplest systems, is the so-called binary interaction parameter characterizing molecular interactions between molecules i and j. When $i = j$, $k_{ij} = 0$. The common practice is to fit k_{ij} so as to represent the vapor–liquid equilibrium data of the mixture under consideration. However, in this paper, in order to obtain a predictive model and to define the PPR78 model (predictive, 1978 PR EOS), k_{ij}, which depends on temperature, is calculated by a group contribution method. Combining different equations from the past work of Péneloux et al. [16–18], $k_{ij}(T)$ is expressed in terms of group contributions, through the following quite simple expression:

$$k_{ij}(T) = \frac{-\frac{1}{2}\sum_{k=1}^{N_{\mathrm{g}}}\sum_{l=1}^{N_{\mathrm{g}}}(\alpha_{ik} - \alpha_{jk})(\alpha_{il} - \alpha_{jl})A_{kl}\cdot\left(\frac{298.15}{T}\right)^{\left(\frac{B_{kl}}{A_{kl}} - 1\right)} - \left(\frac{\sqrt{a_i(T)}}{b_i} - \frac{\sqrt{a_j(T)}}{b_j}\right)^2}{2\frac{\sqrt{a_i(T)\cdot a_j(T)}}{b_i\cdot b_j}} \tag{5}$$

The PPR78 model is thus defined by Eqs. (2)–(5).

In Eq. (5), T is the temperature, a_i and b_i are simply calculated by Eq. (3). N_{g} is the number of different groups defined by the method (for the time being, six groups are defined and $N_{\mathrm{g}} = 6$). α_{ik} is the fraction of molecule i occupied by group k (occurrence of group k in molecule i divided by the total number of groups present in molecule i). $A_{kl} = A_{lk}$ and $B_{kl} = B_{lk}$ (where k and l are two different groups) are constant parameters determined in this study ($A_{kk} = B_{kk} = 0$). As can be seen, to calculate the k_{ij} parameter between two molecules i and j at a selected temperature, it is necessary to know: the critical temperature of both components ($T_{\mathrm{C}i}$, $T_{\mathrm{C}j}$), the critical pressure of both components ($P_{\mathrm{C}i}$, $P_{\mathrm{C}j}$), the acentric factor of each component (ω_i, ω_j) and the decomposition of each molecule into elementary groups (α_{ik}, α_{jk}).

The six groups which are defined in this study are: group 1 = CH_3, group 2 = CH_2, group 3 = CH, group 4 = C, group 5 = CH_4, i.e. methane, group 6 = C_2H_6, i.e. ethane. The decomposition into groups of the hydrocarbons (linear or branched) is very easy, that is, as simple as possible. No substitution effects are considered. No exceptions are defined. For these six groups, we have to estimate 30 parameters (15 A_{kl} and 15 B_{kl} values). These parameters have been determined in order to minimize the deviations between calculated and experimental VLE data from an extended database (see the next section for more detail) containing 16,341 experimental data points (9186 bubble points, 6995 dew points and 160 mixture critical points). The corresponding A_{kl} and B_{kl} values (expressed in Pa) are summarized in Table 1. An example of k_{ij} calculation may be found in Appendix A.

It is important to note that many investigators perform phase equilibria measurements on binary systems at different temperatures. In this case, in order to correlate the data with a cubic EOS (PR76, PR78, SRK, etc.) and classical mixing rules (quadratic on a and linear on b), it is advised to use Eq. (6) (see below) and to fit the two parameters A_{12} and B_{12} on the available experimental data. By doing so, the k_{ij} will become temperature dependent and more accurate results will be obtained than by fitting a constant k_{ij} value. Eq. (6) is similar to Eq. (5) except that each molecule has been considered as a single group:

Table 1
Group interaction parameters: ($A_{kl} = A_{lk}$)/Pa and ($B_{kl} = B_{lk}$)/Pa

	CH_3 (group 1)	CH_2 (group 2)	CH (group 3)	C (group 4)	CH_4 (group 5)	C_2H_6 (group 6)
CH_3 (group 1)	0	–	–	–	–	–
CH_2 (group 2)	$A_{12} = 74.81 \times 10^6$ $B_{12} = 165.7 \times 10^6$	0	–	–	–	–
CH (group 3)	$A_{13} = 261.5 \times 10^6$ $B_{13} = 388.8 \times 10^6$	$A_{23} = 51.47 \times 10^6$ $B_{23} = 79.61 \times 10^6$	0	–	–	–
C (group 4)	$A_{14} = 396.7 \times 10^6$ $B_{14} = 804.3 \times 10^6$	$A_{24} = 88.53 \times 10^6$ $B_{24} = 315.0 \times 10^6$	$A_{34} = -305.7 \times 10^6$ $B_{34} = -250.8 \times 10^6$	0	–	–
CH_4 (group 5)	$A_{15} = 32.94 \times 10^6$ $B_{15} = -35.00 \times 10^6$	$A_{25} = 36.72 \times 10^6$ $B_{25} = 108.4 \times 10^6$	$A_{35} = 145.2 \times 10^6$ $B_{35} = 301.6 \times 10^6$	$A_{45} = 263.9 \times 10^6$ $B_{45} = 531.5 \times 10^6$	0	–
C_2H_6 (group 6)	$A_{16} = 8.579 \times 10^6$ $B_{16} = -29.5 \times 10^6$	$A_{26} = 31.23 \times 10^6$ $B_{26} = 84.76 \times 10^6$	$A_{36} = 174.3 \times 10^6$ $B_{36} = 352.1 \times 10^6$	$A_{46} = 333.2 \times 10^6$ $B_{46} = 203.8 \times 10^6$	$A_{56} = 13.04 \times 10^6$ $B_{56} = 6.863 \times 10^6$	0

$$k_{12}(T) = \frac{A_{12} \cdot \left(\frac{298.15}{T}\right)^{\left(\frac{B_{12}}{A_{12}}-1\right)} - (\delta_1 - \delta_2)^2}{2\delta_1\delta_2} \quad (6)$$

$$\text{with : } \delta_i = \frac{\sqrt{a_i(T)}}{b_i}$$

2.2. On the temperature dependence of the k_{ij} parameter

It is accepted today that the binary interaction parameter k_{ij} depends on temperature. This temperature dependence has been described by a few authors. The very good paper by Coutinho et al. [24] gives an interesting review of the different publications dealing with this subject. The same authors [24] find a theoretical explanation for the temperature dependence of the k_{ij} parameter. They conclude that the temperature dependence of the k_{ij} is quadratic with respect to the inverse temperature ($1/T$). Using Eq. (5), it is simple to plot k_{ij} versus temperature for a given binary system. Fig. 1 presents plots of k_{ij} with respect to the reduced temperature of the heavy *n*-alkane for three binary systems: methane/propane, methane/*n*-hexane and methane/*n*-decane. The shapes of the curves are similar to the ones published by Coutinho et al. [24]. At low temperature, k_{ij} is a decreasing function of temperature. With increasing the temperature, the k_{ij} reaches a minimum and then increases again. The minimum is located at a reduced temperature close to 0.55, independent of the binary system. The minimum moves to $T_R = 0.6$ for the system methane/*n*-C_{30} (results not shown in Fig. 1). From Fig. 1, it can be concluded that k_{ij} depends quite strongly on temperature.

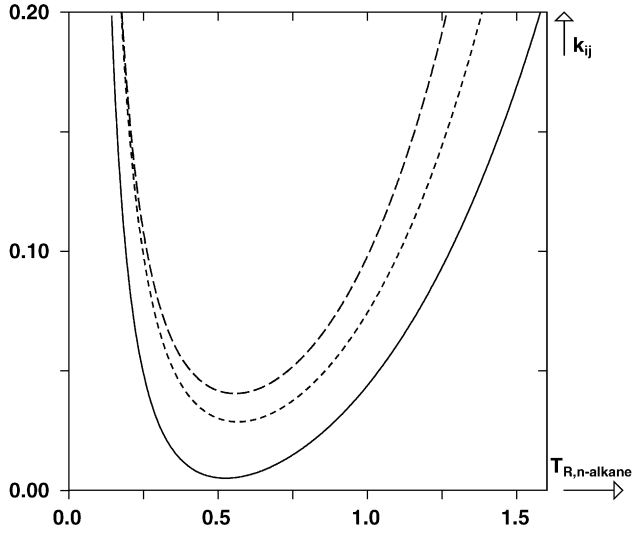

Fig. 1. Temperature dependence of estimated binary interaction parameters (k_{ij}) by means of Eq. (5). Solid line: methane/propane system. Short dashed line: methane/*n*-hexane system. Long dashed line: methane/*n*-decane system. In abscissa, T_R is the reduced temperature of the heavy *n*-alkane (respectively, propane, *n*-hexane, *n*-decane).

2.3. Trends of the k_{ij} parameter with respect to hydrocarbon size

The paper by Coutinho et al. [24] shows that the k_{ij} for CO_2/saturated hydrocarbon mixtures decreases with increasing size difference. Moreover, k_{ij} parameters for CO_2/aromatic systems and for CO_2/monoalkene mixtures increase slightly with molecular size. These authors cannot find any physical explanation for this behavior. By using the

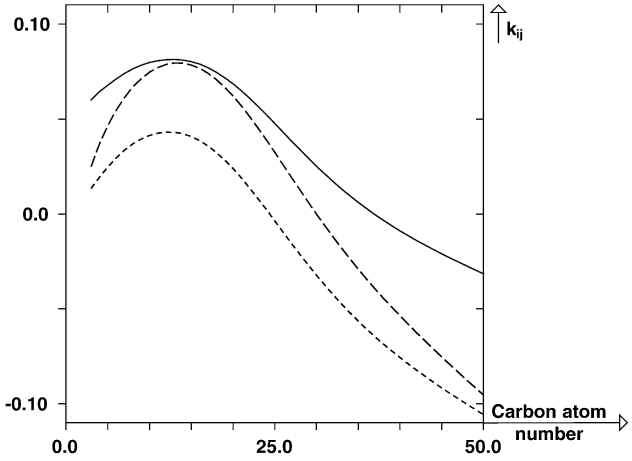

Fig. 2. Calculated values for k_{ij} between methane and linear *n*-alkane (from *n*-C_3 to *n*-C_{50}) at different reduced temperatures of the *n*-alkane. Solid line: $T_R = 0.3$. Short dashed line: $T_R = 0.6$. Long dashed line: $T_R = 0.9$.

Table 2
List of the 28 pure components used in this study

Component	Short name
Methane	1
Ethane	2
Propane	3
n-Butane	4
Isobutane	2m3
n-Pentane	5
2-Methyl butane	2m4
2,2-Dimethyl propane	22m3
n-Hexane	6
2-Methyl pentane	2m5
3-Methyl pentane	3m5
2,2-Dimethyl butane	22m4
2,3-Dimethyl butane	23m4
n-Heptane	7
2-Methyl hexane	2m6
2,4-Dimethyl pentane	24m5
n-Octane	8
2-Methyl heptane	2m7
2,2,4-Trimethyl pentane	224m5
n-Nonane	9
2-Methyl octane	2m8
2,2,5-Trimethyl hexane	225m6
n-Decane	10
n-Undecane	11
n-Dodecane	12
n-Tetradecane	14
n-Hexadecane	16
n-Eicosane	20

PPR78 model developed in this paper, the trends of the k_{ij} parameter with respect to hydrocarbon carbon number can be calculated easily. In Fig. 2, it is shown how k_{ij} varies for the CH_4/*n*-alkane systems when *n* (the hydrocarbon carbon number) varies between 3 and 50. Three curves are plotted in Fig. 2, corresponding to three different values of the reduced temperature of the heavy alkane. Whatever the reduced temperature, the k_{ij} increases first, reaches a maximum (for a carbon number close to 14) and then decreases with increasing carbon number. Therefore, for slightly asymmetric systems, k_{ij} increases with respect to hydrocarbon size, but the reverse behavior appears for highly asymmetric systems (carbon number higher than 14).

3. Database and reduction procedure

Table 2 presents the list of pure components used in this study. The pure fluid physical properties (T_C, P_C and ω) used in this study originate from Poling et al. [31]. Because such data are only available up to eicosane (n-C_{20}), we have limited our database to systems containing hydrocarbons lighter than eicosane.

Table 3 shows the sources of the binary experimental data used in our evaluations along with the temperature, pressure and composition range for each binary system. The data have been used as *P*, *T*, *x* or *P*, *T*, *y* measurements, i.e. the liquid or gas phase composition for a given temperature and pressure.

If, for a given system, *P*, *T*, *x* and *y* are known, we considered that two experimental points are available: a bubble point (*P*, *T*, *x*) and a dew point (*P*, *T*, *y*). Moreover, some mixture critical points (critical pressures P_{Cm} and critical compositions x_C for a given temperature) have been added to our database. Most of the data available in the open literature (9186 bubble points and 6995 dew points) have been collected. Some experimental points were obviously wrong and they have been deleted. Not all the available mixture critical points have been included in our database, but only 160. This procedure reduces the influence on the regressed interaction parameters of data where the equation of state is probably less accurate (we will, however, demonstrate that the PPR78 model enables us to predict the critical locus of binary systems very accurately). Our database includes VLE data on 92 binary systems.

A flash algorithm has been used to perform VLE calculations (for a selected binary system and a given *T* and *P*, we have found the composition of the liquid (*x*) and gas phase (*y*) in equilibrium). According to the phase rule, the critical point of a binary system is monovariant. Therefore, to compute a mixture critical pressure and composition, what you need is to fix the temperature to the experimental critical temperature and to predict P_{Cm} and X_C. The 30 parameters (15 A_{kl} and 15 B_{kl}) given in Table 1 are those which minimize the following objective function:

$$F_{obj} = \frac{F_{obj,bubble} + F_{obj,dew} + F_{obj,crit.\ comp} + F_{obj,crit.\ pressure}}{n_{bubble} + n_{dew} + n_{crit} + n_{crit}} \tag{7}$$

$$\begin{cases} F_{obj,bubble} = 100 \sum_{i=1}^{n_{bubble}} 0.5\left(\frac{|\Delta x|}{x_{1,exp}} + \frac{|\Delta x|}{x_{2,exp}}\right)_i \\ \text{with } |\Delta x| = |x_{1,exp} - x_{1,cal}| = |x_{2,exp} - x_{2,cal}|, \\ F_{obj,dew} = 100 \sum_{i=1}^{n_{dew}} 0.5\left(\frac{|\Delta y|}{y_{1,exp}} + \frac{|\Delta y|}{y_{2,exp}}\right)_i \\ \text{with } |\Delta y| = |y_{1,exp} - y_{1,cal}| = |y_{2,exp} - y_{2,cal}|, \\ F_{obj,crit.\ comp} = 100 \sum_{i=1}^{n_{crit}} 0.5\left(\frac{|\Delta x_C|}{x_{C1,exp}} + \frac{|\Delta x_C|}{x_{C2,exp}}\right)_i \\ \text{with } |\Delta x_C| = |x_{C1,exp} - x_{C1,cal}| = |x_{C2,exp} - x_{C2,cal}|, \\ F_{obj,crit.\ pressure} = 100 \sum_{i=1}^{n_{crit}} \left(\frac{|P_{Cm,exp} - P_{Cm,cal}|}{P_{Cm,exp}}\right)_i \end{cases}$$

where n_{bubble}, n_{dew} and n_{crit} are the number of bubble points, dew points and mixture critical points, respectively. x_1 is the mole fraction in the liquid phase of the most volatile component and x_2 the mole fraction of the heaviest component (it is obvious that $x_2 = 1 - x_1$). Similarly, y_1 is the mole fraction in the gas phase of the most volatile component and y_2 the mole fraction of the heaviest component (it is obvious that $y_2 = 1 - y_1$). x_{C1} is the critical mole fraction of the most volatile component and x_{C2} the critical mole fraction of the heaviest component. P_{Cm} is the binary critical pressure.

Table 3
Binary systems database

Binary system (1st compd.–2nd compd.)	Temperature range (K)	Pressure range (bar)	x_1 range (1st compd. liquid mole fraction)	y_1 range (1st compd. gas mole fraction)	Number of bubble points (T, P, x)	Number of dew points (T, P, y)	Number of binary critical points (T_{Cm}, P_{Cm}, x_C)	References
1–2	90.69–283.15	0.04–66.57	0.0060–0.9956	0.0279–1.0000	336	312	0	[32–42]
1–3	114.10–360.93	0.42–101.63	0.0049–0.9990	0.0276–1.0000	325	322	12	[38,43–46]
1–4	144.26–410.93	1.38–132.59	0.0029–0.9829	0.1110–0.9999	370	370	21	[47–51]
1–2m3	110.00–377.59	0.78–117.88	0.0020–0.9810	0.0300–0.9980	136	123	12	[52–54]
1–5	176.21–460.93	1.38–171.33	0.0004–0.9715	0.0070–0.9999	662	651	40	[55–61]
1–22m3	298.15–410.93	12.13–150.99	0.0510–0.8287	0.2800–0.9554	32	32	0	[55,62]
1–2m4	344.26–449.82	27.58–151.07	0.0040–0.6330	0.0340–0.8850	50	50	0	[55,63]
1–6	182.46–423.15	1.37–201.50	0.0094–0.8191	0.4420–1.0000	300	233	1	[64–68]
1–3m5	298.15–373.15	5.07–30.40	0.0089–0.1440	0.7292–0.9787	24	20	0	[69]
1–7	183.15–510.93	6.89–248.83	0.0132–0.8940	0.2060–0.9997	290	137	8	[59,70–73]
1–8	223.15–423.15	10.13–279.49	0.0330–0.8200	0.7870–0.9990	90	90	2	[74,75]
1–224m5	295.00–295.00	69.90–173.30	0.3415–0.6448	–	4	0	0	[76]
1–9	223.15–423.15	10.05–323.22	0.0329–0.8850	0.8600–1.0000	158	39	4	[73,77,78]
1–225m6	298.15–373.15	69.51–91.40	–	0.9834–0.9987	0	9	0	[79]
1–10	244.26–583.05	1.38–365.45	0.0016–0.8586	0.1828–0.9999	383	230	0	[68,80–84]
1–12	255.28–374.05	13.30–494.50	0.0615–0.8721	0.9135–0.9966	95	7	0	[68,85,86]
1–14	320.64–432.67	27.00–489.20	0.1050–0.8170	–	94	0	0	[87]
1–16	290.00–703.55	20.29–703.46	0.0697–0.9270	0.3097–0.9972	118	41	0	[88–90]
1–20	323.20–573.15	9.50–106.90	0.0427–0.3500	0.9595–0.9993	35	10	0	[91,92]
2–3	127.59–363.16	0.00–51.71	0.0006–0.9986	0.0045–0.9986	414	414	7	[35,38,93–98]
2–4	235.37–419.26	1.61–56.55	0.0200–0.9957	0.1000–0.9970	341	374	0	[93,98–102]
2–2m3	203.15–401.70	0.05–54.50	0.0211–0.9600	0.0431–0.9788	72	63	18	[42,103–105]
2–5	277.59–444.26	2.45–68.26	0.0048–0.9778	0.0385–0.9960	103	64	5	[106,107]
2–6	298.15–449.82	1.72–79.01	0.0150–0.9200	0.0900–0.9886	91	43	3	[108–110]
2–7	234.80–539.82	3.45–88.18	0.0030–0.9800	0.0030–0.9950	263	294	5	[111–113]
2–8	273.15–373.15	4.05–68.00	0.0470–0.9840	0.8987–0.9990	78	76	0	[114,115]
2–224m5	287.16–346.65	1.01–66.79	0.0260–0.8420	0.9260–0.9710	12	8	0	[116,117]
2–10	277.59–510.93	3.45–118.24	0.0170–0.9950	0.3347–0.9999	187	99	7	[118–120]
2–11	298.15–318.15	11.97–54.27	0.2782–0.9690	–	19	0	0	[121]
2–12	273.15–373.20	3.60–62.82	0.0500–0.9800	–	155	0	0	[122–125]
2–20	280.00–572.85	2.33–167.60	0.0731–0.9901	0.9499–0.9988	172	8	0	[91,126,127]
3–4	260.00–419.65	0.76–42.92	0.0630–0.9410	0.1000–0.9830	167	169	0	[128–130]
3–2m3	266.54–366.48	1.32–38.20	0.0039–0.9919	0.0065–0.9966	47	47	0	[131]
3–5	321.35–461.85	3.34–44.82	0.0040–0.9820	0.0120–0.9960	238	241	0	[129,132,133]
3–2m4	273.15–453.15	0.51–45.80	0.0350–0.9830	0.0570–0.9845	83	83	6	[134]
3–6	273.15–492.75	0.54–49.50	0.1000–0.9176	0.1000–0.9176	129	90	0	[135,136]
3–22m4	348.15–479.10	2.29–47.01	0.1527–0.9194	0.1527–0.9194	58	98	0	[137]
3–23m4	348.15–489.23	2.00–48.57	0.1516–0.9153	0.1516–0.9153	58	72	0	[137]
3–2m5	348.15–488.06	1.84–48.21	0.1497–0.9190	0.1497–0.9190	62	99	0	[137]
3–3m5	348.15–494.95	1.47–49.37	0.1451–0.8850	0.1451–0.8850	56	82	0	[137]
3–7	338.35–531.85	20.68–51.71	0.1000–0.9090	0.1000–0.9090	78	73	0	[136]
3–8	329.15–559.25	6.89–57.92	0.1000–0.9589	0.1000–0.9589	145	128	0	[138,139]
3–9	376.75–377.15	9.38–34.68	0.2936–0.8543	0.9739–0.9904	5	5	0	[140]
3–10	277.59–510.93	1.72–70.88	0.0190–0.9870	0.3382–0.9999	103	56	3	[140,141]
3–16	273.15–313.15	0.56–12.72	0.0720–0.9370	–	38	0	0	[135]
3–20	279.29–358.56	4.03–32.47	0.2540–0.9497	–	166	0	0	[142]
4–2m3	273.15–373.15	1.07–19.61	0.0370–0.9500	0.0310–0.9380	75	48	0	[143–145]
4–5	298.15–464.45	0.73–37.23	0.0176–0.9000	0.1000–0.9000	113	86	0	[146,147]
4–6	253.15–501.95	0.05–38.61	0.0820–0.9215	0.1000–0.9680	279	199	2	[144,147–149]
4–7	329.09–539.71	2.76–40.68	0.0110–0.9410	0.1000–0.9900	203	218	0	[150]
4–8	339.45–561.65	6.89–43.09	0.1000–0.9461	0.1000–0.9461	109	88	0	[139]
4–10	310.93–510.93	1.72–49.23	0.0324–0.9751	0.3444–0.9999	61	61	3	[151]
4–14	402.03–453.95	4.00–44.03	0.2027–0.9074	–	59	0	0	[87]
5–22m3	253.15–293.15	0.12–1.34	0.1333–0.8649	–	49	0	0	[148]
5–6	298.15–337.35	0.25–1.00	0.0638–0.9458	0.1880–0.9947	50	42	0	[152–154]
5–7	403.71–526.45	10.13–30.61	0.1000–0.9000	0.1700–0.9610	42	42	1	[155,156]
5–8	291.52–433.63	0.06–15.20	0.0220–0.9500	0.2247–0.9993	94	94	0	[154,157]
5–10	317.70–333.70	0.48–1.46	0.2283–0.6824	0.9591–0.9990	16	16	0	[154]
2m4–6	306.89–335.25	1.01–1.01	0.0956–0.7667	0.2522–0.9296	32	32	0	[158]
6–22m4	298.15–298.15	0.23–0.40	0.1051–0.8825	–	9	0	0	[152]

Table 3 (*Continued*)

Binary system (1st compd.–2nd compd.)	Temperature range (K)	Pressure range (bar)	x_1 range (1st compd. liquid mole fraction)	y_1 range (1st compd. gas mole fraction)	Number of bubble points (T, P, x)	Number of dew points (T, P ,y)	Number of binary critical points (T_{Cm}, P_{Cm}, x_C)	References
6–23m4	298.15–298.15	0.21–0.30	0.0979–0.9009	0.0655–0.8559	9	9	0	[152]
6–2m5	283.15–313.15	0.11–0.50	0.0987–0.9129	0.0750–0.8412	53	44	0	[152,159]
6–3m5	283.15–313.15	0.11–0.45	0.0785–0.9169	0.0656–0.8977	57	33	0	[152,159]
6–7	288.35–369.45	0.10–1.01	0.0383–0.9243	0.0852–0.9637	114	32	0	[160–165]
6–24m5	283.15–313.15	0.07–0.36	0.1279–0.9100	0.1836–0.9368	52	52	0	[159]
6–8	288.35–388.35	0.04–1.01	0.0500–0.9500	0.2620–0.9940	75	21	0	[163,166,167]
6–10	308.15–417.95	0.03–1.01	0.0846–0.9028	–	19	0	0	[168,169]
6–11	308.15–308.15	0.02–0.28	0.0792–0.9029	–	12	0	0	[170]
6–12	308.15–308.15	0.02–0.28	0.0751–0.9055	–	12	0	0	[171]
6–16	293.15–333.15	0.00–0.62	0.0282–0.8940	–	78	0	0	[167,172,173]
22m4–16	293.15–293.15	0.07–0.29	0.2100–0.8490	–	10	0	0	[174]
23m4–16	293.15–293.15	0.09–0.22	0.3570–0.8650	–	7	0	0	[174]
2m5–7	318.15–328.15	0.18–0.82	0.0564–0.9543	0.1808–0.9871	42	42	0	[175]
2m5–2m6	493.80–521.60	19.80–30.00	0.1207–0.9080	0.1207–0.9080	23	23	0	[176]
2m5–8	283.15–328.15	0.02–0.82	0.0346–0.9633	0.4056–0.9957	71	64	0	[175,177]
2m5–2m7	498.80–548.40	20.60–30.60	0.1375–0.9206	0.1375–0.9206	18	18	0	[176]
2m5–2m8	501.30–576.30	20.20–30.80	0.1384–0.9272	0.1384–0.9272	22	22	0	[176]
2m5–16	293.15–293.15	0.08–0.19	0.3610–0.8390	–	8	0	0	[174]
3m5–7	308.15–328.15	0.11–0.74	0.0445–0.9499	0.1284–0.9853	63	55	0	[178]
3m5–8	283.15–333.15	0.02–0.88	0.0335–0.9649	0.5646–0.9957	73	59	0	[177,178]
3m5–16	293.15–293.15	0.07–0.18	0.3610–0.8580	–	8	0	0	[174]
7–8	313.85–394.45	0.10–1.01	0.0330–0.9620	0.0720–0.9820	89	32	0	[160,163,179,180]
7–224m5	370.35–372.16	0.96–1.01	0.1888–0.8583	0.2060–0.8160	9	5	0	[160,181]
24m5–8	283.15–313.15	0.01–0.22	0.1037–0.8673	0.4162–0.9800	52	52	0	[177]
2m6–2m7	520.70–552.90	20.70–27.00	0.1301–0.9074	0.1301–0.9074	21	21	0	[176]
2m6–2m8	527.30–578.60	21.50–27.00	0.1270–0.9199	0.1270–0.9199	21	21	0	[176]
8–224m5	371.25–397.30	0.59–1.01	0.1017–0.9568	–	16	0	0	[160,182]
8–10	349.15–392.25	0.20–0.20	0.0080–0.9890	0.0320–0.9980	27	27	0	[183]
8–12	349.35–429.85	0.20–0.20	0.0050–0.9880	0.0560–0.9990	26	26	0	[183]
8–16	298.15–298.15	0.00–0.02	0.1050–0.8971	–	17	0	0	[167]
2m7–2m8	556.40–578.50	20.80–24.90	0.1080–0.9075	0.1080–0.9075	23	23	0	[176]
10–12	393.25–430.55	0.20–0.20	0.0100–0.9810	0.0310–0.9960	26	26	0	[183]
Total number of points					9186	6995	160	

The choice of an objective function is never an easy task. In this study the previously described objective functions were selected for different reasons. Percent deviations and not absolute deviations were selected in order to be able to mix mole fractions and critical pressures data. Moreover, we average the mole fraction percent deviations for components 1 and 2 (see $F_{obj,bubble}$, $F_{obj,dew}$ and $F_{obj,crit.\ comp}$) in order to reduce the influence on the regressed parameters of the very small (or large) mole fractions. As an example if $y_{1,exp} = 0.999$ and $y_{1,calc} = 0.998$, is the model accurate or not? It depends on what you want. Indeed, $\Delta y_1\% = 0.1$ but $\Delta y_2\% = 100\%$. In our approach, the objective function for such a data point would be 50%.

4. Results and discussion

4.1. Results for systems included in the database

For all the data points included in our database, the objective function defined by Eq. (7) is $F_{obj} = 4.73\%$.

The average overall deviation on the liquid phase composition is

$$\bar{\Delta x_1} = \frac{\sum_{i=1}^{n_{bubble}} (|x_{1,exp} - x_{1,cal}|)_i}{n_{bubble}} = 0.011,$$

$$\text{moreover } \frac{F_{obj,bubble}}{n_{bubble}} = 3.77\%$$

The average overall deviation on the gas phase composition is

$$\bar{\Delta y_1} = \frac{\sum_{i=1}^{n_{dew}} (|y_{1,exp} - y_{1,cal}|)_i}{n_{dew}} = 0.0096,$$

$$\text{moreover } \frac{F_{obj,dew}}{n_{dew}} = 5.96\%$$

The average overall deviation on the critical composition is

$$\bar{\Delta x_{C1}} = \frac{\sum_{i=1}^{n_{crit}} (|x_{C1,exp} - x_{C1,cal}|)_i}{n_{crit}} = 0.016,$$

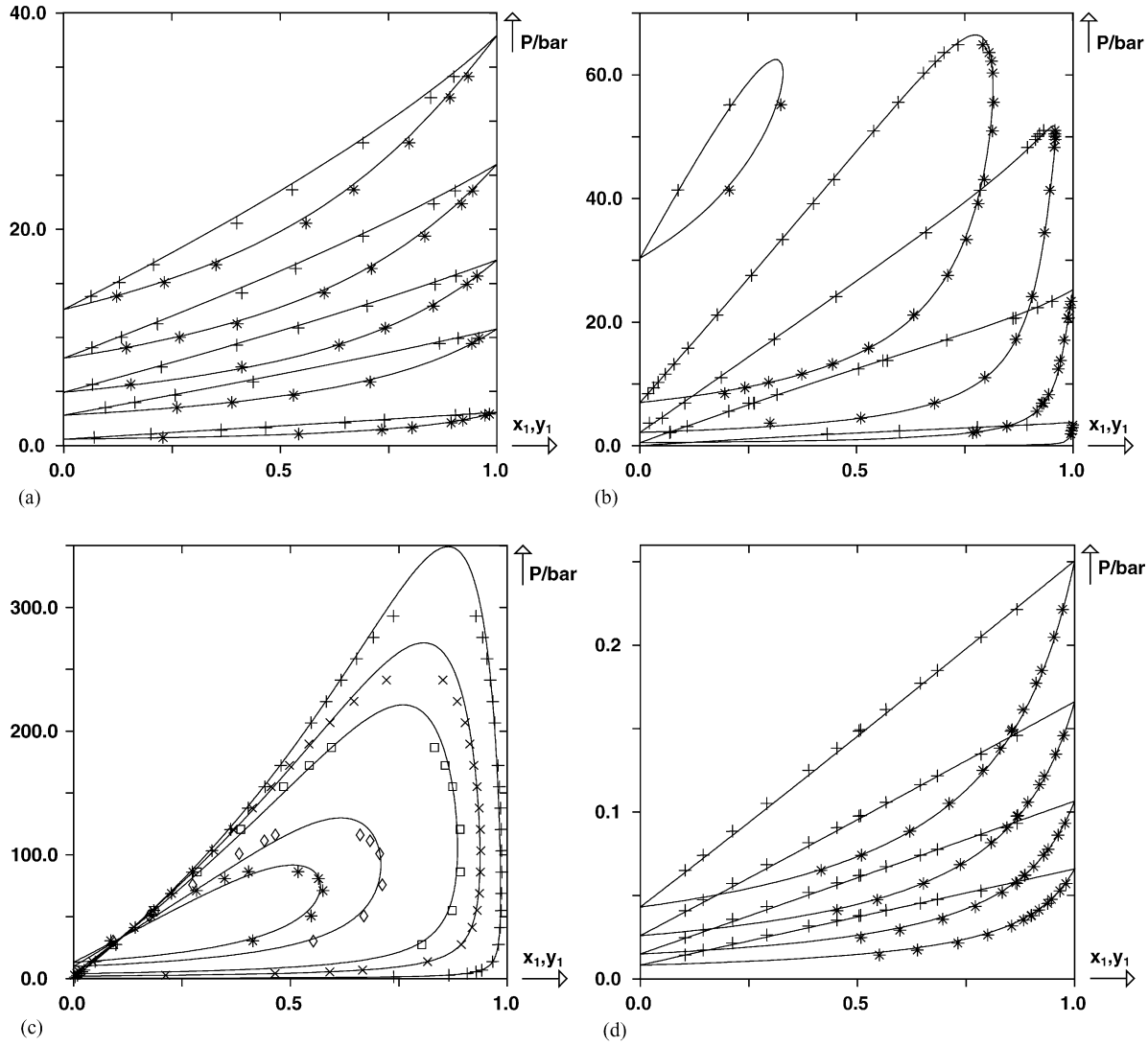

Fig. 3. Prediction of isothermal dew and bubble curves for four binary systems using the PPR78 model. Solid line: predicted curves with the PPR78 model. (a) System propane(1)/*n*-butane(2) at five different temperatures: T_1 = 260.00 K (k_{ij} = 0.0031), T_2 = 303.15 K (k_{ij} = 0.0028), T_3 = 323.10 K (k_{ij} = 0.0027), T_4 = 343.17 K (k_{ij} = 0.0026), T_5 = 363.38 K (k_{ij} = 0.0025). (+) Experimental bubble points, (*) experimental dew points. (b) System methane(1)/ethane(2) at five different temperatures: T_1 = 130.37 K (k_{ij} = 0.0013), T_2 = 172.04 K (k_{ij} = 0.0034), T_3 = 199.93 K (k_{ij} = 0.0049), T_4 = 230.00 K (k_{ij} = 0.0065), T_5 = 283.15 K (k_{ij} = 0.0096). (+) Experimental bubble points, (*) experimental dew points. (c) System methane(1)/*n*-decane(2) at five different temperatures: T_1 = 410.93 K (k_{ij} = 0.044; +, experimental data), T_2 = 477.59 K (k_{ij} = 0.055; ×, experimental data), T_3 = 510.95 K (k_{ij} = 0.062; □, experimental data), T_4 = 563.25 K (k_{ij} = 0.077; ◇, experimental data), T_5 = 583.05 K (k_{ij} = 0.084; *, experimental data). (d) System 2,4-dimethyl pentane(1)/*n*-octane(2) at four different temperatures: T_1 = 283.15 K (k_{ij} = 0.000162), T_2 = 293.15 K (k_{ij} = −0.000501), T_3 = 303.15 K (k_{ij} = −0.001129), T_4 = 313.15 K (k_{ij} = −0.001726). (+) Experimental bubble points, (*) experimental dew points.

$$\text{moreover } \frac{F_{\text{obj,crit. comp}}}{n_{\text{crit}}} = 6.33\%$$

The average overall deviation on the binary critical pressure is

$$\Delta\bar{P}_{\text{C}}\% = \frac{F_{\text{obj,crit. pressure}}}{n_{\text{crit}}} = \frac{100\sum_{i=1}^{n_{\text{crit}}}(|P_{\text{Cm,exp}} - P_{\text{Cm,cal}}|/P_{\text{Cm,exp}})_i}{n_{\text{crit}}} = 4.16\ \%$$

These results clearly indicate that the PPR78 model is a very good predictive model. Figs. 3–5 illustrate for some typical binary systems the accuracy of the proposed model.

Fig. 3a shows the isothermal phase diagrams of a system containing two light components at low pressure: propane(1)/*n*-butane(2). The value of the objective function for the points plotted in this figure is F_{obj} = 4.06 which is close to the value obtained for the whole database. At low temperature, the bubble curve is a straight line, which means that the liquid phase is an ideal solution. By increasing temperature, negative deviations of the ideality appear. The PPR78 model

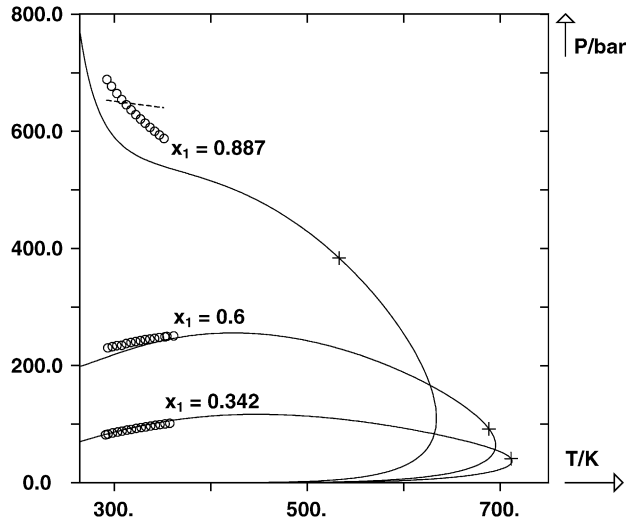

Fig. 4. Solid line: prediction results with the PPR78 model of three isopleths for the $CH_4(1)$ + n-$C_{16}(2)$ system. (+) Calculated critical points with the PPR78 model. Dashed line: prediction with the LCVM model for a selected isopleth. The experimental bubble pressures (◯) are from Glaser et al. [89].

can perfectly reproduce this phenomenon. Moreover, for this system, k_{ij} slightly varies with the temperature.

Fig. 3b shows the isothermal phase diagrams of a system containing two light components at high pressure: methane(1)/ethane(2). The value of the objective function for the points plotted in this figure is F_{obj} = 2.25 which is smaller than the value obtained in the whole database. This is not surprising because methane and ethane are two different groups. Once again, the PPR78 model perfectly reproduces the experimental data points. For this system the k_{ij} at low temperature is seven times smaller than the k_{ij} at high temperature. Selecting temperature dependent k_{ij} is so extremely important.

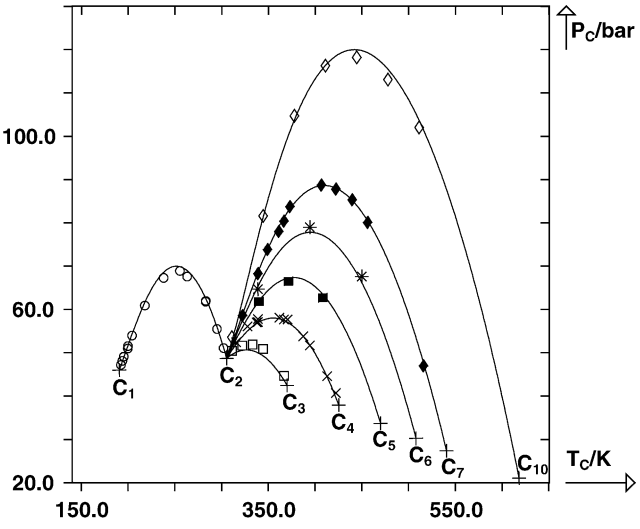

Fig. 5. Prediction of the critical locus of ethane + n-alkane binary mixtures using the PPR78 equation of state. Experimental data (◯, □, ×, ■, *, ♦, ◊) were obtained from the literature [186]. Solid line: predicted critical locus. (+) Pure component (CH_4, C_2H_6, C_3H_8, n-C_4, n-C_5, n-C_6, n-C_7, n-C_{10}) critical point.

Fig. 3c shows the isothermal phase diagrams of an asymmetric binary system at high pressure: methane(1)/n-decane(2). The objective function for the points plotted is F_{obj} = 3.25. For this system, very accurate results are obtained even though the critical region is not perfectly reproduced at low temperature. For this system, the k_{ij} is more or less multiplied by a factor 2 when the temperature rises from 411 to 583 K.

Fig. 3d shows the isothermal phase diagrams of a binary system containing a branched alkane: 2,4-dimethyl pentane(1)/n-octane(2). For such a system, the liquid phase is an ideal solution and the k_{ij} is very close to zero. It is positive at low temperature and negative at higher temperature. It increases by a factor 10 between 283 and 313 K.

Fig. 4 shows three isopleths (constant composition P, T diagram) for the system $CH_4(1)$ + n-$C_{16}(2)$. When the amount of methane is not very high, say x_1 lower than 0.7, the PPR78 model can accurately predict the bubble-point pressures as a function of temperature. The results obtained with the LCVM model [184] are equivalent (they are not shown in Fig. 4). By increasing the amount of CH_4, larger deviations appear simultaneously for the PPR78 model and the LCVM model (see Fig. 4). The PPR78 model underestimates by about 10–11% the bubble-point pressures. Such a deviation is systematic, which means that the slope of the curve predicted with the PPR78 model is very close to the experimental slope. The deviations obtained with the LCVM model are quite similar but the predicted slope is completely wrong. As shown in Fig. 4, for extrapolation purposes at high temperature, the PPR78 model seems much better than the LCVM model.

The prediction of phase equilibria of binary mixtures in the critical region is an important problem because the shape of the critical locus gives necessary basic information about the topology of phase behavior. For this reason, it has been decided to predict the critical locus of ethane + n-alkane binary mixtures by using the PPR78 equation of state. The homologous series of ethane + n-alkane (at least up to n-decane) mixtures exhibit a continuous vapor–liquid critical curve between the pure components. This corresponds to type I behavior in the classification scheme of van Konynenburg and Scott [185]. A comparison between theory and experiment is illustrated in Fig. 5. It is here important to notice that

Table 4
Composition of Turek's oil and deviation between experimental and predicted bubble-point pressures with the PPR78 model

Temperature	T_1 = 322.0 K	T_2 = 338.7 K
Experimental bubble pressure	$P_{1,exp}$ = 101.97 bar	$P_{2,exp}$ = 107.49 bar
Predicted bubble pressure with the PPR78 model	$P_{1,cal}$ = 100.63 bar	$P_{2,cal}$ = 107.27 bar
Absolute deviation	ΔP_1 = 1.34 bar	ΔP_2 = 0.22 bar
Relative deviation	ΔP_1% = 1.32	ΔP_2% = 0.21

Synthetic oil composition (mol%): CH_4, 34.67; C_2H_6, 3.13; C_3H_8, 3.96; n-C_4, 5.95; n-C_5, 4.06; n-C_6, 3.06; n-C_7, 4.95; n-C_8, 4.97; n-C_{10}, 30.21; n-C_{14}, 5.04.

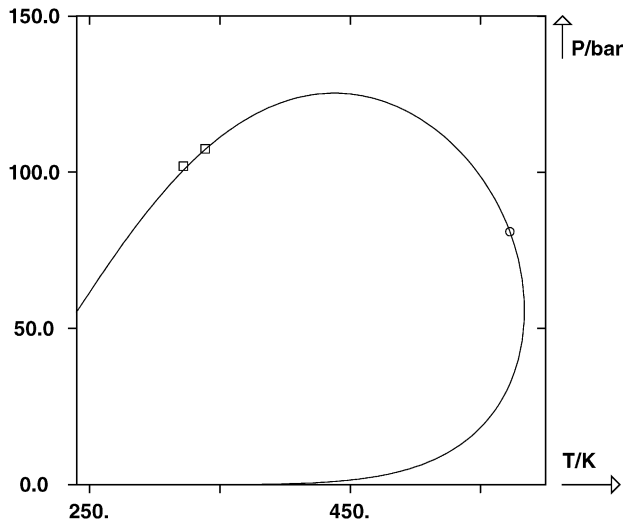

Fig. 6. Solid line: (P, T) phase envelope of Turek's synthetic oil mixture predicted with the PPR78 model. (□) Experimental bubble-point pressures; (◯) predicted critical point.

most of the data points shown in Fig. 5 were in fact not included in our database. The overall quality of predictions obtained from the PPR78 model are surprisingly good even when the carbon number of the *n*-alkane increases. Indeed, in many papers, it is said that cubic EOS are inherently inaccurate near the critical point. We here give proof that, by using temperature dependent k_{ij}, it is possible to predict with high accuracy the critical locus of binary systems (at least for type I systems).

4.2. Results for systems not included in the database for which the critical parameters and the acentric factor are known

4.2.1. Study of a synthetic petroleum fluid

In 1984, Turek et al. [187] measured the bubble-point pressure of a mixture (a synthetic crude oil) containing 10 *n*-alkanes ranging from methane to *n*-C_{14} at two different temperatures. For all these hydrocarbons, the critical parameters and the acentric factor are known from

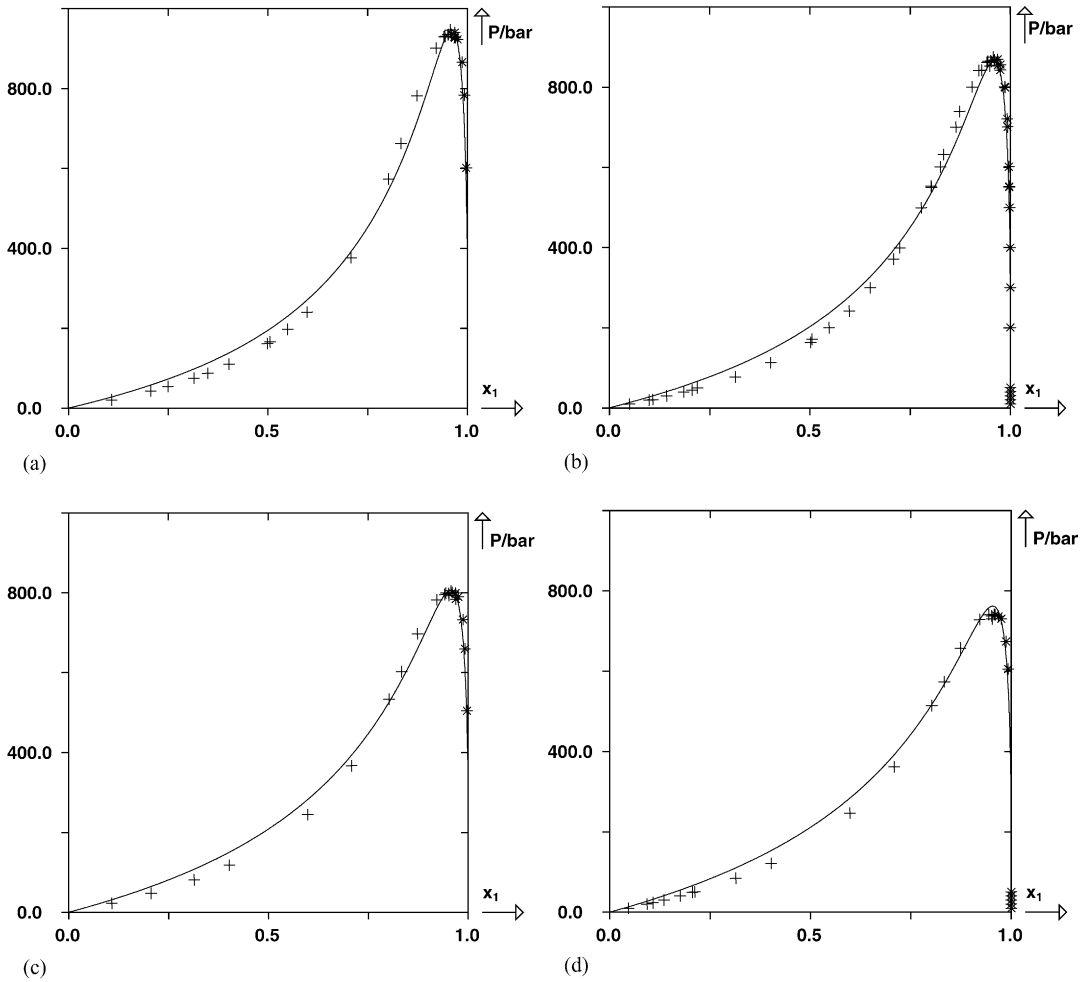

Fig. 7. Prediction of isothermal dew and bubble curves for the hyperbaric binary system $CH_4(1)/n\text{-}C_{24}(2)$ using the PPR78 EOS. Experimental dew point pressures (*) and bubble-point pressures (+) were obtained from the literature: (a) $T = 350$ K and $k_{ij} = 0.045$; (b) $T = 374 \pm 1$ K and $k_{ij} = 0.042$; (c) $T = 400$ K and $k_{ij} = 0.040$; (d) $T = 424 \pm 1$ K and $k_{ij} = 0.039$.

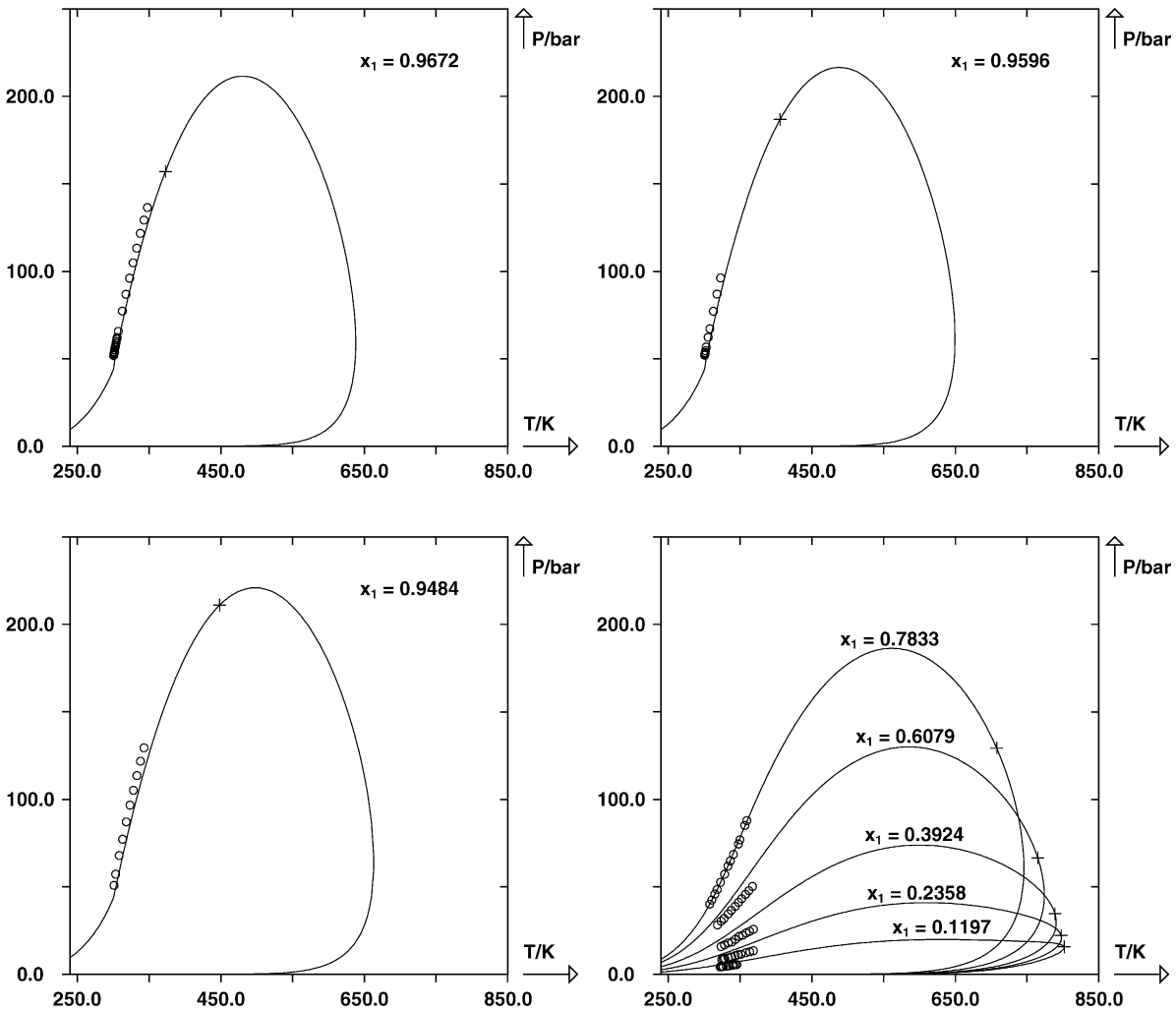

Fig. 8. Solid line: prediction results with the PPR78 model of eight isopleths for the $C_2H_6(1)$ + n-$C_{24}(2)$ system. (+) Calculated critical points with the PPR78 model; (◯) experimental bubble pressures.

experiments. It has thus been decided to use the proposed PPR78 model to predict these two bubble-point pressures. The results and the composition of the oil are given in Table 4 and may be seen in Fig. 6. From this table, it can be concluded that the accuracy of the PPR78 model (0.78 bar on average, i.e. 0.77%) is identical to the experimental uncertainty.

4.2.2. *The hyperbaric CH_4/n-C_{24} system*

The asymmetry of the CH_4/n-C_{24} system, the very high saturation pressures (>800 bar) and the wide range of conditions that data cover make this system very attractive to test the capability of cubic equations of state. The critical properties and the acentric factor of the n-tetracosane (n-C_{24}) are not known from experiments. However, because such a system was widely studied, it is possible to find in the literature values which are currently used in cubic equations of state [188–190]. The values we have used in this study are T_C = 805 K, P_C = 10.5 bar and ω = 1.05. A comparison of prediction with the PPR78 model and experiment [191–193] is illustrated in Fig. 7. From this figure, it is clear that the PPR78 model can perfectly predict VLE of very asymmetric systems. For this system and by using the LCVM model, Stamataki et al. [189] report an average deviation of 14% on the bubble-point pressures. It is thus obvious from Fig. 7 that better results are obtained with the PPR78 model.

4.2.3. *The C_2H_6/n-C_{24} system*

In 1987, Peters et al. [194] measured 104 bubble-point pressures for the system ethane(1) + n-$C_{24}(2)$. The amount of ethane (mol%) ranges from 11.97% to 96.72%. The PPR78 model has been able to predict these 104 values with an average deviation of 5.4 bar. When the amount of ethane is very high (between 85 and 95%), the PPR78 model slightly underestimates the bubble pressures. When the amount of ethane is close to 75%, a perfect agreement between predicted and experimental data is observed. When the amount of ethane is smaller, the PPR78 model overestimates the bubble-point pressures. In all cases, the slope of the predicted curve is correct. All these results may be seen in Fig. 8 (the k_{ij} varies between 0.025 at low temperature to 0.19 at high temperature).

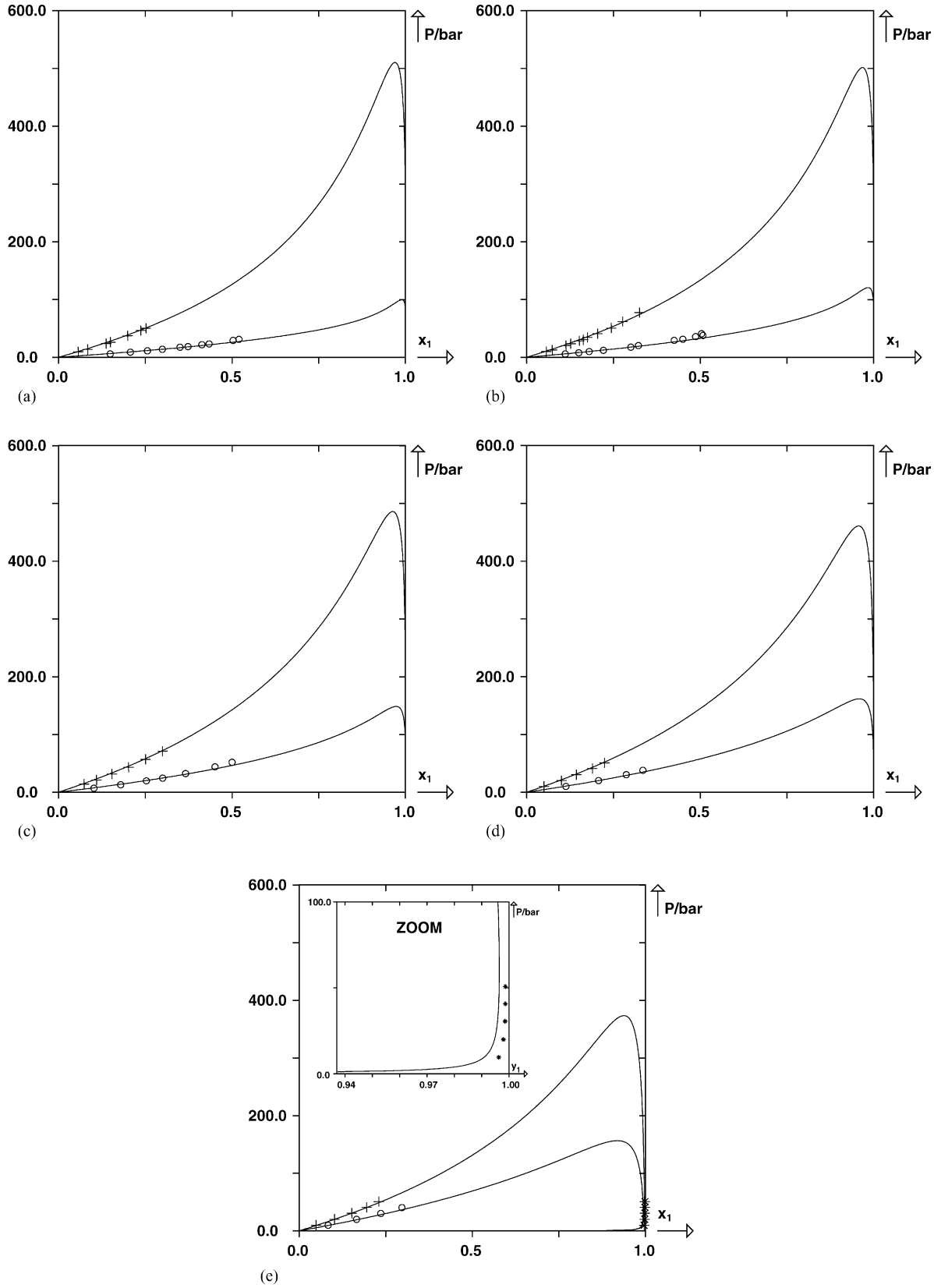

Fig. 9. Prediction of isothermal dew and bubble curves for the binary systems CH_4/*n*-C_{28} and C_2H_6/*n*-C_{28} using the PPR78 EOS. Experimental dew point pressures (* for the CH_4/*n*-C_{28}) and bubble-point pressures (+ for the CH_4/*n*-C_{28} and ◯ for the C_2H_6/*n*-C_{28}) were obtained from the literature. (a) Systems CH_4/*n*-C_{28} (k_{ij} = 0.020) and C_2H_6/*n*-C_{28} (k_{ij} = −0.052) at T = 348.2 K. (b) Systems CH_4/*n*-C_{28} (k_{ij} = 0.015) and C_2H_6/*n*-C_{28} (k_{ij} = −0.057) at T = 373.20 K. (c) Systems CH_4/*n*-C_{28} (k_{ij} = 0.0083) and C_2H_6/*n*-C_{28} (k_{ij} = −0.064) at T = 423.2 K. (d) Systems CH_4/*n*-C_{28} (k_{ij} = 0.0047) and C_2H_6/*n*-C_{28} (k_{ij} = −0.068) at T = 473.3 K. (e) Systems CH_4/*n*-C_{28} (k_{ij} = 0.0053) and C_2H_6/*n*-C_{28} (k_{ij} = −0.063) at T = 573.2 K.

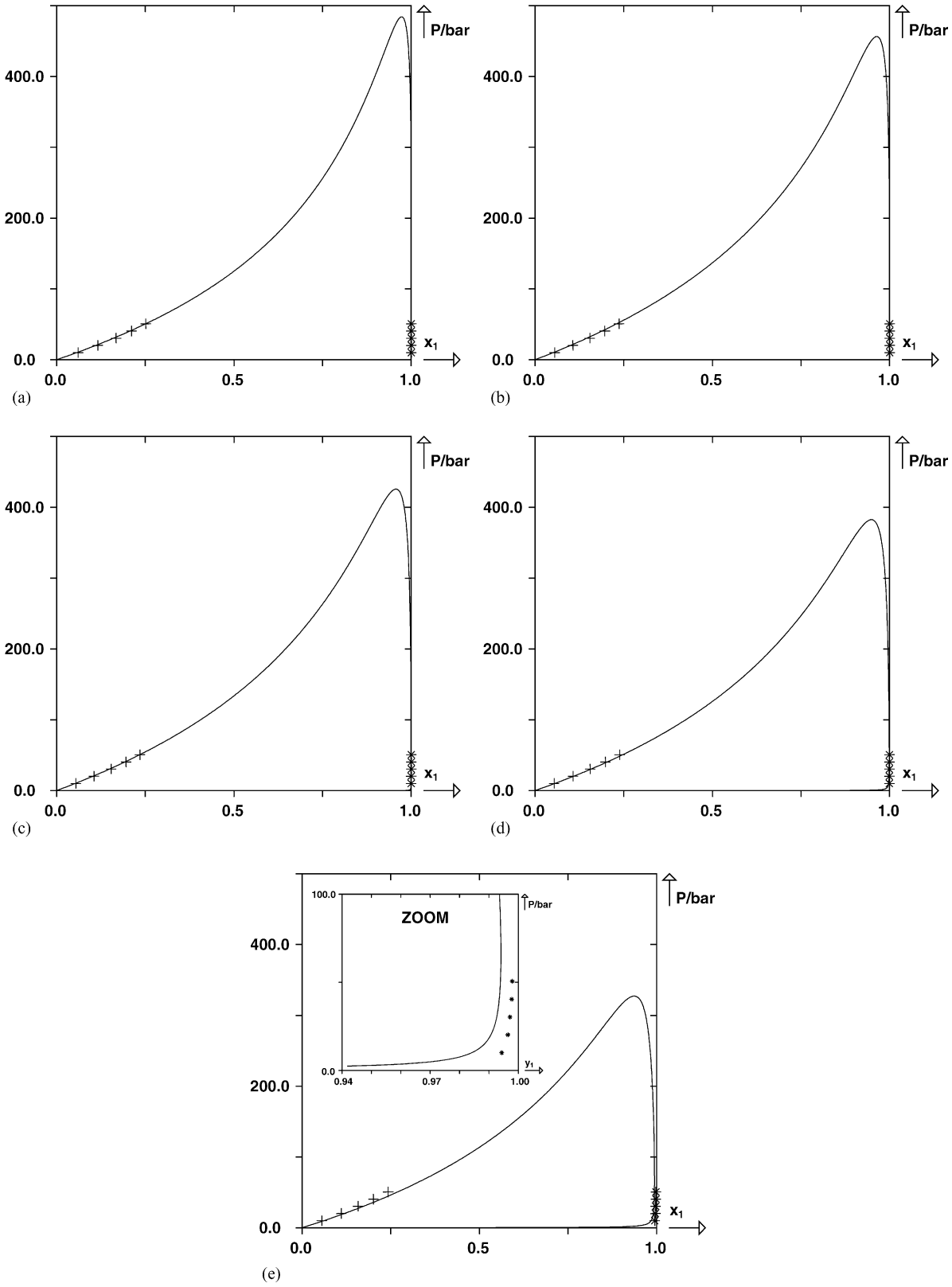

Fig. 10. Prediction of isothermal dew and bubble curves for the binary system $CH_4(1)/n\text{-}C_{32}(2)$ using the PPR78 EOS. Experimental dew point pressures (*) and bubble-point pressures (+) were obtained from the literature. (a) System $CH_4/n\text{-}C_{32}$ at $T = 373.15$ K ($k_{ij} = 0.0058$). (b) System $CH_4/n\text{-}C_{32}$ at $T = 473.15$ K ($k_{ij} = -0.0079$). (c) System $CH_4/n\text{-}C_{32}$ at $T = 523.15$ K ($k_{ij} = -0.0107$). (d) System $CH_4/n\text{-}C_{32}$ at $T = 573.15$ K ($k_{ij} = -0.0112$). (e) System $CH_4/n\text{-}C_{32}$ at $T = 623.15$ K ($k_{ij} = -0.0094$).

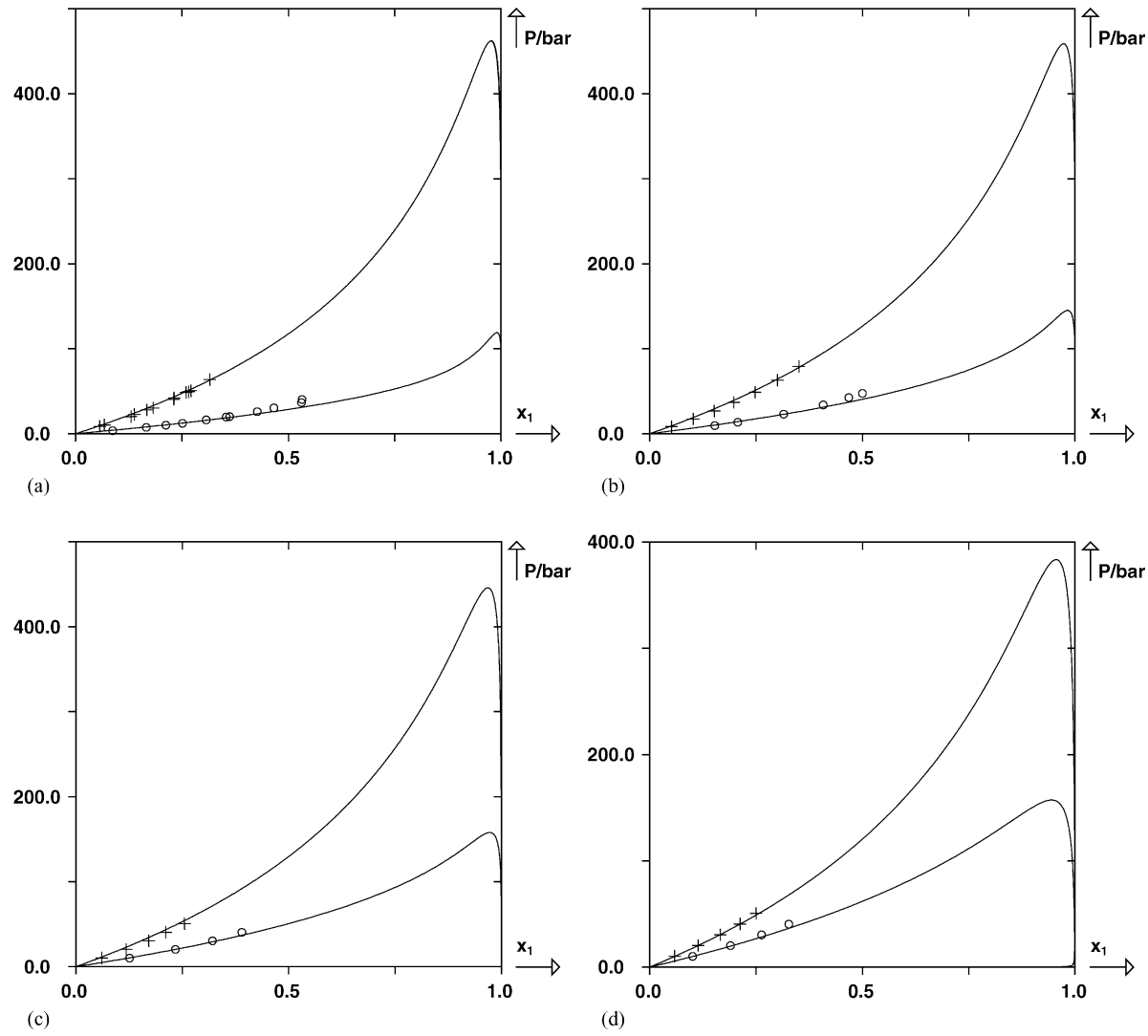

Fig. 11. Prediction of isothermal dew and bubble curves for the binary systems CH_4/*n*-C_{36} and C_2H_6/*n*-C_{36} using the PPR78 EOS. Experimental bubble-point pressures (+ for the CH_4/*n*-C_{36} and ◯ for the C_2H_6/*n*-C_{36}) were obtained from the literature. (a) Systems CH_4/*n*-C_{36} ($k_{ij} = -0.00351$) and C_2H_6/*n*-C_{36} ($k_{ij} = -0.0865$) at $T = 373.15$ K. (b) Systems CH_4/*n*-C_{36} ($k_{ij} = -0.0134$) and C_2H_6/*n*-C_{36} ($k_{ij} = -0.0973$) at $T = 423.20$ K. (c) Systems CH_4/*n*-C_{36} ($k_{ij} = -0.0203$) and C_2H_6/*n*-C_{36} ($k_{ij} = -0.1052$) at $T = 473.1$ K. (d) Systems CH_4/*n*-C_{36} ($k_{ij} = -0.0271$) and C_2H_6/*n*-C_{36} ($k_{ij} = -0.1099$) at $T = 573.1$ K.

4.3. Results for systems not included in the database for which the critical parameters and the acentric factor are unknown

When the critical parameters and the acentric factors are unknown, a new problem arises: which correlation or which group contribution method (GCM) should be used to estimate these values? The answer to this question is very difficult. Indeed, the various estimation methods lead to differences which can easily reach 10% and sometimes much more for very heavy components (100% difference in the critical pressure of heavy *n*-alkanes is common). Moreover, these differences are of great importance in VLE predictions. An interesting discussion of this problem is to be found in a paper by Stamataki and Tassios [190]. These authors explain that a given estimation method may lead to accurate results for a given compound but not for another one. Let us recall that the aim of this paper is to propose a GCM to estimate the binary interaction parameters. However, if T_C, P_C and ω are not correct, even with the best k_{ij}, poor results will be obtained. In order to test the accuracy of our GCM, it has thus been decided to adopt a strategy aimed at estimating T_C, P_C and ω. Poling et al. [31] state that the GCM developed by Gani and co-workers to estimate T_C, P_C and ω is probably the most accurate [195,196]. For heavy hydrocarbons, it was decided to use this method, assuming that its accuracy is of about 10%. Doing so, for each heavy hydrocarbon used in this section, we have defined T_C, P_C and ω by:

$$T_C\,(\text{to be used}) = \lambda T_{C,\text{GANI}}, \quad P_C\,(\text{to be used}) = \lambda P_{C,\text{GANI}},$$
$$\omega\,(\text{to be used}) = \lambda \omega_{\text{GANI}} \ \text{ with } 0.9 < \lambda < 1.1 \tag{8}$$

The parameter λ which is the same for the three properties is determined in order to have the best prediction of VLE

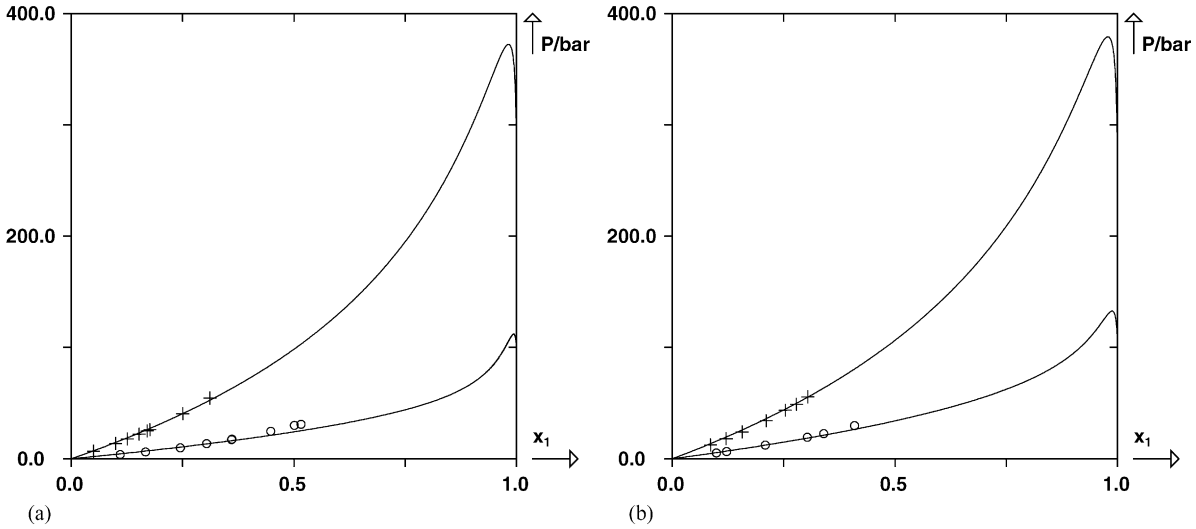

Fig. 12. Prediction of isothermal dew and bubble curves for the binary systems CH_4/*n*-C_{44} and C_2H_6/*n*-C_{44} using the PPR78 EOS. Experimental bubble-point pressures (+ for the CH_4/*n*-C_{44} and ◯ for the C_2H_6/*n*-C_{44}) were obtained from the literature. (a) Systems CH_4/*n*-C_{44} (k_{ij} = −0.0319) and C_2H_6/*n*-C_{44} (k_{ij} = −0.1290) at T = 373.2 K. (b) Systems CH_4/*n*-C_{44} (k_{ij} = −0.0454) and C_2H_6/*n*-C_{44} (k_{ij} = −0.1437) at T = 423.2 K.

experimental data. In other words, λ is adjusted to the experimental data (it was simply found by trial and errors). We did not use a correction on a single property in order to have the same covolume *b* as the one calculated by the original Gani's method (here the ration T_C/P_C is unchanged).

4.3.1. The CH_4/*n*-C_{28} and C_2H_6/*n*-C_{28} systems

The critical properties and the acentric factor of the *n*-C_{28} alkane are those determined by Gani's GCM multiplied by λ = 0.973. By, doing so, we have found T_C = 801.0 K, P_C = 7.0 bar and ω = 1.158. The experimental data available in the literature [92,126,197] at five different temperatures for the two systems have been predicted with the PPR78 EOS. Due to their high asymmetry, these systems are quite difficult to predict. However, accurate results have been obtained with our model. For the system CH_4/*n*-C_{28}, k_{ij} is always positive. It ranges from 0.02 to 0.005 when the temperature rises from 348 to 573 K. The reverse phenomenon takes places for the system C_2H_6/*n*-C_{28}. For this system, the predicted k_{ij} is always negative. It ranges from −0.05 to −0.07 when the temperature varies from 348 to 573 K. These results are graphically illustrated in Fig. 9.

4.3.2. The CH_4/*n*-C_{32} (*n*-dotriacontane) system

For the *n*-dotriacontane properties (T_C, P_C and ω), the fitted λ value was 0.970. The used parameters are thus: T_C = 822.81 K, P_C = 5.98 bar and ω = 1.292. For this system, five (*P*, *T*, *x*, *y*) data points were measured at five different temperatures by Huang et al. [193]. As shown in Fig. 10, the PPR78 model can perfectly predict these data.

4.3.3. The CH_4/*n*-C_{36} and C_2H_6/*n*-C_{36} systems

For the *n*-hexatriacontane properties (T_C, P_C and ω), the value λ = 0.966 has been selected. This value is very close to what has been obtained for the *n*-C_{28} and the *n*-C_{32}. The used parameters are thus: T_C = 840.68 K, P_C = 5.2034 bar and ω = 1.4179. For these systems, VLE data points were measured at four different temperatures by different authors [92,126,198]. As shown in Fig. 11, the PPR78 model can predict these data accurately. All the k_{ij} are negative and can have large values especially for the C_2H_6/*n*-C_{36} system.

4.3.4. The CH_4/*n*-C_{44} and C_2H_6/*n*-C_{44} systems

For the *n*-tetratetracontane properties (T_C, P_C and ω), the value λ = 0.936 has been selected. The used parameters are thus: T_C = 849.50 K, P_C = 4.0322 bar and ω = 1.6126. For

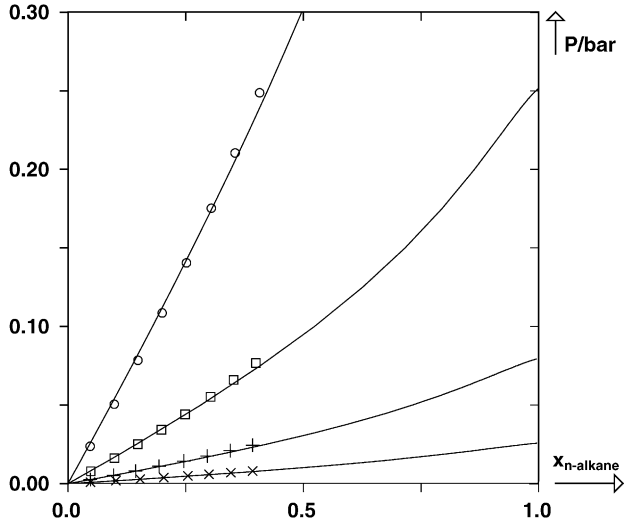

Fig. 13. Prediction of isothermal dew and bubble curves for binary systems containing squalane at T = 303.15 K using the PPR78 EOS. Experimental bubble-point pressures were obtained from the literature. (◯) System *n*-C_5/squalane (k_{ij} = −0.0622). (□) System *n*-C_6/squalane (k_{ij} = −0.0598). (+) System *n*-C_7/squalane (k_{ij} = −0.0562). (×) System *n*-C_8/squalane (k_{ij} = −0.0514).

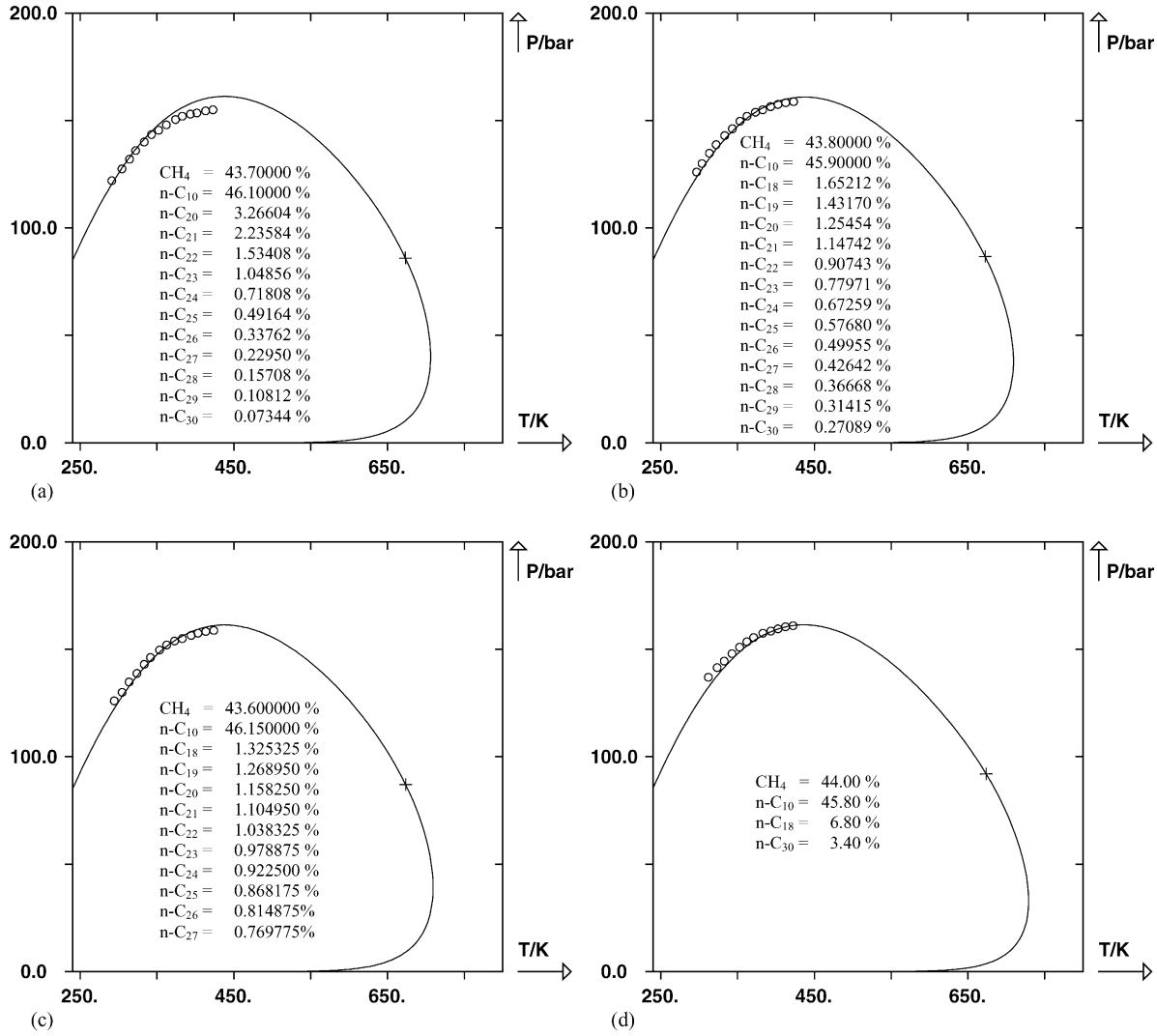

Fig. 14. Prediction of bubble-point pressures of four different synthetic fluids with the PPR78 EOS. The compositions in mol% are given in each figure. (a) $\Delta P\% = 2.0$, (b) $\Delta P\% = 1.1$, (c) $\Delta P\% = 1.1$, (d) $\Delta P\% = 1.2$.

these systems VLE data points were measured at two different temperatures by different authors [92,126]. As shown in Fig. 12, the PPR78 model can predict these data accurately. The same behavior as for the systems containing *n*-C_{36} is observed: the k_{ij} values are negative and can have large values especially for the system containing ethane.

4.3.5. The n-alkanes/squalane (2,6,10,15,19,23-hexamethyl tetracosane) systems at 303.15 K

In 1973, Ashworth [199] measured at $T = 303.15$ K, the bubble-point pressures of systems containing *n*-alkane (from *n*-C_5 to *n*-C_8) and squalane ($C_{30}H_{62}$). These data have been predicted with the PPR78 model and the excellent results obtained can be seen in Fig. 13. For the squalane properties (T_C, P_C and ω), the value $\lambda = 1.000$ has been selected which means that the original values by Gani et al. have been used (the parameters are $T_C = 819.863$ K, $P_C = 6.6010$ bar and $\omega = 1.16983$).

4.3.6. The four synthetic fluids (CH_4/n-decane/multi-paraffins mixtures) of Daridon et al.

In 1996, Daridon et al. [200] measured a total of 54 bubble-point pressures on four mixtures containing up to 15 components. These four mixtures contain CH_4 + *n*-decane + *n*-paraffins ranging from *n*-C_{18} to *n*-C_{30}. Such data are thus particularly interesting to test the PPR78 EOS and to make comparisons with other well-know purely predictive EOS/g^E models. For the *n*-alkanes heavier than *n*-C_{20} and different from *n*-C_{24} and *n*-C_{28} which have been previously studied, the same λ value has been determined. We have selected $\lambda_{Cn} = 1.077$ ($n = 21, 22, 23, 25, 26, 27, 29, 30$). The corresponding ($P$, T) phase envelopes predicted with the PPR78 EOS can be seen in Fig. 14. Such fluids were also studied by Boukouvalas et al. [184], who report an average percent deviation on the 54 bubble-point pressures equal to 4.2% for the LCVM model and of 39.2% for the MHV2 model, respectively. When the PPR78 model is used, this deviation is 1.4%. This means that our results are three times better than those obtained with the

LCVM model and 28 times better than those obtained with MHV2. In order to be fair, let us recall that in this study the λ parameter has been fitted.

5. Conclusion

A group contribution method allowing the estimation of the temperature dependent binary interaction parameters ($k_{ij}(T)$) for the widely used Peng–Robinson equation of state has been developed. A key point in our approach is that the k_{ij} between two components i and j is a function of temperature (T), of the critical temperatures (T_{Ci} and T_{Cj}), of the critical pressures (P_{Ci}, P_{Cj}) and of the acentric factors (ω_i, ω_j) of the two components. This means that no additional properties besides those required by the EOS itself (T_C, P_C, ω) are required.

In this paper, six groups are defined: CH_3, CH_2, CH, C, CH_4 (methane), and C_2H_6 (ethane) which means that it is possible to estimate the k_{ij} for any mixture of saturated hydrocarbons (*n*-alkanes and branched alkanes) whatever the temperature.

The results obtained in this study are in many cases very accurate in both the sub-critical and critical regions and often better than those obtained with the best EOS/g^E models. This paper thus gives proof that by using temperature dependent k_{ij}, it is possible to predict with high accuracy:

1) the critical locus of binary systems (at least for type I systems),
2) the phase behavior of asymmetric systems.

To conclude, because the λ parameter defined by Eq. (8) is very often close to unity, the GCM developed by Gani and coworkers to estimate T_C, P_C and ω of heavy hydrocarbons is a very powerful tool which combines well with the proposed GCM.

List of symbols

$a(T)$	temperature dependent function of the equation of state
A_{kl}, B_{kl}	constant parameters allowing the calculation of the binary interaction parameters
b	covolume
E_{ij}	binary interaction parameter of the Van Laar excess function
g^E	excess Gibbs energy
k_{ij}	binary interaction parameter
m	shape parameter
P	pressure
P_C	critical pressure
R	ideal gas constant
T	temperature
T_C	critical temperature
v	volume
x_i, y_i, z_i	mole fraction

Greek letters

α_{ik}	fraction occupied by group k in the molecule i
ω	acentric factor

Acknowledgments

The French Petroleum Company TOTAL and more particularly Doctors François Montel, Danielle Morel, Patrick Gouel and Pierre Duchet-Suchaux are gratefully acknowledged for sponsoring this research.We also thank Professor Evelyne Neau from the French University of the Mediterranean warmly for the helpful discussions we had while doing this research.

Appendix A. Example of k_{ij} calculation

An example of k_{ij} calculation is given to show how easy the method is. For example, let us calculate the binary interaction parameter between propane (1) and *n*-butane (2) at $T = 303.15$ K. This simple calculation is divided into five tasks.

- *Task 1*: decomposition of the molecules into elementary groups.
  Component 1 (propane) contains 2 groups 1 (CH_3), 1 group 2 (CH_2) and 0 group 3, 4, 5 and 6. The total number of groups present in molecule 1 is thus $N_{g_1} = 1 + 2 = 3$. Component 2 (*n*-butane) contains 2 groups 1 (CH_3), 2 groups 2 (CH_2) and 0 group 3, 4, 5 and 6. The total number of groups present in molecule 2 is thus $N_{g_2} = 2 + 2 = 4$.
- *Task 2:* calculation of the α parameters.
  The fraction of molecule 1 (propane) occupied by group 1 (CH_3) is

$$\alpha_{11} = \frac{\text{number of group 1 in molecule 1}}{\text{total number of groups in molecule 1}} = \frac{2}{N_{g_1}} = \frac{2}{3}$$

  The fraction of molecule 1 occupied by group 2 (CH_2) is $\alpha_{12} = 1/3$.
  Because molecule 1 contains 0 group 3, 4, 5 and 6, we have $\alpha_{13} = \alpha_{14} = \alpha_{15} = \alpha_{16} = 0$.
  The fraction of molecule 2 (*n*-butane) occupied by group 1 (CH_3) is

$$\alpha_{21} = \frac{\text{number of group 1 in molecule 2}}{\text{total number of groups in molecule 2}} = \frac{2}{N_{g_2}} = \frac{2}{4}$$

  The fraction of molecule 2 occupied by group 2 (CH_2) is $\alpha_{22} = 2/4$.
  Because molecule 2 contains 0 group 3, 4, 5 and 6, we have $\alpha_{23} = \alpha_{24} = \alpha_{25} = \alpha_{26} = 0$.

- *Task 3*: calculation of the double sum appearing in Eq. (5). We want to compute k_{12} which means that $i = 1$ and $j = 2$. Thus, with $N_g = 6$, the double sum (DS) can be written as:

$$\mathrm{DS} = -\frac{1}{2}\sum_{k=1}^{6}\sum_{l=1}^{6}(\alpha_{1k}-\alpha_{2k}) \times (\alpha_{1l}-\alpha_{2l})A_{kl}\left(\frac{298.15}{T}\right)^{((B_{kl}/A_{kl})-1)}$$

Taking into account that $\alpha_{13} = \alpha_{14} = \alpha_{15} = \alpha_{16} = 0$ and that $\alpha_{23} = \alpha_{24} = \alpha_{25} = \alpha_{26} = 0$, we have:

$$\begin{aligned}\mathrm{DS} &= -\frac{1}{2}\left[(\alpha_{11}-\alpha_{21})(\alpha_{12}-\alpha_{22}) \times A_{12}\left(\frac{298.15}{T}\right)^{((B_{12}/A_{12})-1)} + (\alpha_{12}-\alpha_{22}) \times (\alpha_{11}-\alpha_{21})A_{21}\left(\frac{298.15}{T}\right)^{((B_{21}/A_{21})-1)}\right] \\ &= -(\alpha_{11}-\alpha_{21})(\alpha_{12}-\alpha_{22}) \times A_{12}\left(\frac{298.15}{T}\right)^{((B_{12}/A_{12})-1)}\end{aligned}$$

With $\alpha_{11} = 2/3$, $\alpha_{12} = 1/3$, $\alpha_{21} = \alpha_{22} = 1/2$, $A_{12} = 74.81 \times 10^6\ Pa$, $B_{12} = 165.7 \times 10^6\ Pa$, and $T = 303.15$ K, one obtains $DS = 2.036 \times 10^6\ Pa$.

- *Task 4*: calculation of a_i and b_i ($i = 1, 2$)

Taking : $\begin{cases} T_{C,1} = 369.83\,\mathrm{K} \\ P_{C,1} = 42.48 \times 10^5\,\mathrm{Pa} \\ \omega_1 = 0.152 \end{cases}$

and $\begin{cases} T_{C,2} = 425.12\,\mathrm{K} \\ P_{C,2} = 37.96 \times 10^5\,\mathrm{Pa} \\ \omega_2 = 0.200 \end{cases}$

one obtains

$$\begin{cases} a_1\,(T = 303.15) = 1.1371\ \mathrm{S.I.} \\ a_2\,(T = 303.15) = 1.8361\ \mathrm{S.I.} \end{cases}$$

and $\begin{cases} b_1 = 5.6313 \times 10^{-5}\,\mathrm{m^3\,mol^{-1}} \\ b_2 = 7.2440 \times 10^{-5}\,\mathrm{m^3\,mol^{-1}} \end{cases}$

- *Task 5*: calculation of k_{12}

Using Eq. (5), we obtain $k_{\text{propane}/n\text{-butane}}\,(T = 303.15\ K) = 0.0028$.

References

[1] J. Gmehling, Fluid Phase Equilib. 210 (2003) 161–173.
[2] J.P. Novak, J. Matous, J. Pick, Liquid–Liquid Equilibrium , Elsevier, Amsterdam, 1987.
[3] A. Fredenslund, R.L. Jones, J.M. Prausnitz, AIChE J. 21 (6) (1975) 1086–1099.
[4] J. Vidal, Chem. Eng. Sci. 33 (6) (1978) 787–791.
[5] M.J. Huron, J. Vidal, Fluid Phase Equilib. 3 (4) (1979) 255–271.
[6] M.M. Michelsen, Fluid Phase Equilib. 60 (1–2) (1990) 213–219.
[7] S. Dahl, A. Fredenslund, P. Rasmussen, Ind. Eng. Chem. Res. 30 (8) (1991) 1936–1945.
[8] B.L. Larsen, P. Rasmussen, A. Fredenslund, Ind. Eng. Chem. Res. 26 (11) (1987) 2274–2286.
[9] T. Holderbaum, J. Gmehling, Fluid Phase Equilib. 70 (2–3) (1991) 251–265.
[10] H.K. Hansen, P. Rasmussen, A. Fredenslund, M. Schiller, J. Gmehling, Ind. Eng. Chem. Res. 30 (10) (1991) 2352–2355.
[11] D.S.H. Wong, S.I. Sandler, AIChE J. 38 (5) (1992) 671–680.
[12] H. Orbey, S.I. Sandler, D.S.H. Wong, Fluid Phase Equilib. 85 (1993) 41–54.
[13] C. Boukouvalas, N. Spiliotis, P. Coutsikos, N. Tzouvaras, D. Tassios, Fluid Phase Equilib. 92 (1994) 75–106.
[14] E.C. Voutsas, C.J. Boukouvalas, N.S. Kalospiros, D.P. Tassios, Fluid Phase Equilib. 116 (1996) 480–487.
[15] H. Orbey, S.I. Sandler, Fluid Phase Equilib. 132 (1–2) (1997) 1–14.
[16] E. Rauzy, A. Péneloux, Int. J. Thermophys. 7 (3) (1986) 635–646.
[17] A. Péneloux, W. Abdoul, E. Rauzy, Fluid Phase Equilib. 47 (2–3) (1989) 115–132.
[18] W. Abdoul, E. Rauzy, A. Péneloux, Fluid Phase Equilib. 68 (1991) 47–102.
[19] H.V. Kehiaian, K. Sosnkowska-Kehiaian, R. Hryniewicz, J. Chim. Phys. Phys. Chim. Biol. 68 (6) (1971) 922–934.
[20] B. Carrier, M. Rogalski, A. Péneloux, Ind. Eng. Chem. Res. 27 (9) (1988) 1714–1721.
[21] E. Rauzy, Ph.D. Dissertation. The French University of Aix-Marseille II, 1982.
[22] D.B. Robinson, D.Y. Peng, The characterization of the heptanes and heavier fractions for the GPA Peng–Robinson programs, Gas processors association, Research Report RR-28, 1978 (booklet only sold by the GPA, Gas Processors Association).
[23] V.I. Harismiadis, A.Z. Panagiotopoulos, D.P. Tassios, Fluid Phase Equilib. 94 (1994) 1–18.
[24] J.A.P. Coutinho, G.M. Kontogeorgis, E.H. Stenby, Fluid Phase Equilib. 102 (1) (1994) 31–60.
[25] W. Gao, R.L. Robinson, K.A.M. Gasem, Fluid Phase Equilib. 213 (1–2) (2003) 19–37.
[26] A. Kordas, K. Magoulas, S. Stamataki, D. Tassios, Fluid Phase Equilib. 112 (1) (1995) 33–44.
[27] G. Avlonitis, G. Mourikas, S. Stamataki, D. Tassios, Fluid Phase Equilib. 101 (1994) 53–68.
[28] A. Kordas, K. Tsoutsouras, S. Stamataki, D. Tassios, Fluid Phase Equilib. 93 (1994) 141–166.
[29] G. Gao, J.L. Daridon, H. Saint-Guirons, P. Xans, F. Montel, Fluid Phase Equilib. 74 (1992) 85–93.
[30] D.Y. Peng, D.B. Robinson, Ind. Eng. Chem. Fundam. 15 (1) (1976) 59–64.
[31] B.E. Poling, J.M. Prausnitz, J.P. O'Connell, The Properties of Gases and Liquids , 5th ed., McGraw Hill, 2000.
[32] R.C. Miller, A.J. Kidnay, M.J. Hiza, J. Chem. Thermodyn. 9 (1977) 167–178.
[33] I. Wichterle, R. Kobayashi, J. Chem. Eng. Data 17 (1972) 9–12.
[34] I. Wichterle, R. Kobayashi, J. Chem. Eng. Data 17 (1972) 13–18.
[35] A.R. Price, Thesis, Rice Institute, Houston, Texas, 1957.
[36] J. Davalos, W.R. Anderson, R.E. Phelps, A.J. Kidnay, J. Chem. Eng. Data 21 (1976) 81–84.
[37] M.K. Gupta, G.C. Gardner, M.J. Hegarty, A.J. Kidnay, J. Chem. Eng. Data 25 (1980) 313–318.
[38] A.R. Price, R. Kobayashi, J. Chem. Eng. Data 4 (1959) 40–52.
[39] M.S.W. Wei, T.S. Brown, A.J. Kidnay, E.D. Sloan, J. Chem. Eng. Data 40 (1995) 726–731.
[40] E.J.S. Gomes de Azevedo, J.C.G. Calado, Fluid Phase Equilib. 49 (1989) 21–34.
[41] G.M. Wilson, Adv. Cryog. Eng. 20 (1975) 164–171.

[42] V.G. Skripka, I.E. Nikitina, L.A. Zhdanovich, A.G. Sirotin, O.A. Ben'aminovich, Gazov. Prom-st 15 (1970) 35–36.
[43] D.P.L. Poon, B.C.Y. Lu, Adv. Cryog. Eng. 19 (1974) 292–299.
[44] I. Wichterle, R. Kobayashi, J. Chem. Eng. Data 17 (1972) 4–9.
[45] H.H. Reamer, B.H. Sage, W.N. Lacey, Ind. Eng. Chem. 42 (1950) 534–539.
[46] W.W. Akers, J.F. Burns, W.R. Fairchild, Ind. Eng. Chem. 46 (1954) 2531–2534.
[47] L.C. Kahre, J. Chem. Eng. Data 19 (1974) 67–71.
[48] B.H. Sage, B.L. Hicks, W.N. Lacey, Ind. Eng. Chem. 32 (1940) 1085–1092.
[49] L.R. Roberts, R.H. Wang, A. Azarnoosh, J.J. McKetta, J. Chem. Eng. Data (1962) 7.
[50] D.G. Elliot, R.J.J. Chen, P.S. Chappelear, R. Kobayashi, J. Chem. Eng. Data 19 (1974) 71–77.
[51] H.C. Wiese, J. Jacobs, B.H. Sage, J. Chem. Eng. Data 15 (1970) 82–91.
[52] R.H. Olds, B.H. Sage, W.N. Lacey, Ind. Eng. Chem. 34 (1942) 1008–1013.
[53] S.D. Barsuk, V.G. Skripka, O.A. Ben'yaminovich, Gazov. Promst. 15 (1970) 38–41.
[54] W.M. Haynes, J. Chem. Thermodyn. 15 (1983) 903–911.
[55] B. Williams, N.W. Prodany, J. Chem. Eng. Data 16 (1971) 1–6.
[56] B.H. Sage, H.H. Reamer, R.H. Olds, W.N. Lacey, Ind. Eng. Chem. 34 (1942) 1108–1117.
[57] T.C. Chu, R.J.J. Chen, P.S. Chappelear, R. Kobayashi, J. Chem. Eng. Data 21 (1976) 41–44.
[58] L.C. Kahre, J. Chem. Eng. Data 20 (1975) 363–367.
[59] K. Nagahama, S. Suzuki, S. Oba, M. Hirata, Sekiyu Gakkaishi 28 (1985) 63–69.
[60] V.M. Berry, B.H. Sage, Natl. Stand. Ref. Data Ser. (U.S., Natl. Bur. Stand.), 1970, pp. 32–105.
[61] H.S. Taylor, G.W. Wald, B.H. Sage, W.N. Lacey, Oil Gas J. 38 (1939) 46–50.
[62] B.L. Rogers, J.M. Prausnitz, J. Chem. Thermodyn. 3 (1971) 211–216.
[63] E.H. Amick Jr., W.B. Johnson, B.F. Dodge, Chem. Eng. Prog. Symp. Ser. 48 (1952) 65–72.
[64] J. Shim, J.P. Kohn, J. Chem. Eng. Data 7 (1962) 3–8.
[65] R.D. Gunn, J.J. McKetta, N. Ata, AIChE J. 20 (1974) 347–353.
[66] Y.N. Lin, R.J.J. Chen, P.S. Chappelear, R. Kobayashi, J. Chem. Eng. Data 22 (1977) 402–408.
[67] H. Marteau, J. Obriot, A. Barreau, V. Ruffier Meray, E. Behar, Fluid Phase Equilib. 129 (1997) 285–305.
[68] S. Srivastan, N.A. Darwish, N.A. Gasem, R.L. Robinson Jr., J. Chem. Eng. Data 37 (1992) 516–520.
[69] J.P. Kohn, J.H.S. Haggin, J. Chem. Eng. Data 12 (1967) 313–315.
[70] H.L. Chang, L.J. Hurt, R. Kobayashi, AIChE J. 12 (1966) 1212–1216.
[71] H.H. Reamer, B.H. Sage, W.N. Lacey, Ind. Eng. Chem. Data Ser. 1 (1956) 29–42.
[72] J.P. Kohn, AIChE J. 7 (1961) 514–518.
[73] H. Schlichting, R. Langhorst, H. Knapp, Fluid Phase Equilib. 84 (1993) 143–163.
[74] J.P. Kohn, W.F. Bradish, J. Chem. Eng. Data 9 (1964) 5–8.
[75] A.S. Velikovskii, G.S. Stepanova, Ya. Vybornova, I. Gazov. Prom-st 9 (1964) 1–6.
[76] S. Peramanu, B.P. Pruden, Can. J. Chem. Eng. 75 (1997) 535–543.
[77] L.M. Shipman, J.P. Kohn, J. Chem. Eng. Data 11 (1966) 176–180.
[78] P. Rousseaux, D. Richon, H. Renon, Fluid Phase Equilib. 11 (1983) 153–168.
[79] S.G. D'Avila, B.K. Kaul, J.M. Prausnitz, J. Chem. Eng. Data 21 (1976) 488–491.
[80] K.T. Koonce, R. Kobayashi, J. Chem. Eng. Data 9 (1964) 490–501.
[81] J.M. Beaudoin, J.P. Kohn, J. Chem. Eng. Data 12 (1967) 189–191.
[82] H.-M. Lin, H.M. Sebastian, J.J. Simnick, K.-C. Chao, J. Chem. Eng. Data 24 (1979) 146–149.
[83] H.H. Reamer, R.H. Olds, B.H. Sage, W.N. Lacey, Ind. Eng. Chem. 34 (1942) 1526–1531.
[84] M.P.W.M. Rijkers, M. Malais, C.J. Peters, J. de Swaan Arons, Fluid Phase Equilib. 71 (1992) 143–168.
[85] J.F. Arnaud, Ph.D. Dissertation, France, 1995.
[86] M.P.W.M. Rijkers, V.B. Maduro, C.J. Peters, J. de Swaan Arons, Fluid Phase Equilib. 72 (1992) 309–324.
[87] V.V. de Leeuw, T.W. de Loos, H.A. Kooijman, J. de Swaan Arons, Fluid Phase Equilib. 73 (1992) 285–321.
[88] H.-M. Lin, H.M. Sebastian, K.-C. Chao, J. Chem. Eng. Data 25 (1980) 252–254.
[89] M. Glaser, C.J. Peters, H.J. Van der Kooi, R.N. Lichtenthaler, J. Chem. Thermodyn. 17 (1985) 803–815.
[90] M.P.W.M. Rijkers, C.J. Peters, J. de Swaan Arons, Fluid Phase Equilib. 85 (1993) 335–345.
[91] S.H. Huang, H.M. Lin, K.C. Chao, J. Chem. Eng. Data 33 (1988) 145–147.
[92] N.A. Darwish, J. Fathikalajahi, K.A. Gasem, R.L. Robinson, J. Chem. Eng. Data 38 (1993) 44–48.
[93] P. Uchytil, I. Wichterle, Fluid Phase Equilib. 15 (1983) 209–217.
[94] D.E. Maschke, G. Thodos, J. Chem. Eng. Data 7 (1962) 232–234.
[95] L. Djordjevich, R.A. Budenholzer, J. Chem. Eng. Data 15 (1970) 10–12.
[96] J. Miksovsky, I. Wichterle, Collect. Czech. Chem. Commun. 40 (1975) 365–370.
[97] C.J. Blanc, J.C.B. Setler, J. Chem. Eng. Data 33 (1988) 111–115.
[98] Q.C. Alisdair, K. Stead, J. Chem. Thermodyn. 20 (1988) 413–428.
[99] V. Lhotak, I. Wichterle, Fluid Phase Equilib. 6 (1981) 229–235.
[100] J.G. Dingrani, G. Thodos, Can. J. Chem. Eng. 56 (1978) 616–623.
[101] V.S. Mehra, G. Thodos, J. Chem. Eng. Data 10 (1965) 307–309.
[102] W.B. Kay, Ind. Eng. Chem. 32 (1940) 353–357.
[103] G.J. Besserer, D.B. Robinson, J. Chem. Eng. Data 18 (1973) 301–304.
[104] G. Kaminishi, C. Yokoyama, S. Takahashi, Sekiyu Gakkaishi 29 (1986) 32–37.
[105] T.W. de Loos, H.J. van der Kooi, P.L. Ott, J. Chem. Eng. Data 31 (1986) 166–168.
[106] H.H. Reamer, B.H. Sage, W.N. Lacey, J. Chem. Eng. Data 5 (1960) 44–50.
[107] H.H. Reamer, V. Berry, B.H. Sage, J. Chem. Eng. Data 2 (1961) 184–191.
[108] K. Ohgaki, F. Sano, T. Katayama, J. Chem. Eng. Data 21 (1976) 55–58.
[109] E.J. Zais, I.H. Silberberg, J. Chem. Eng. Data 15 (1970) 253–256.
[110] K.A. Gasem, A.M. Raff, N.A. Darwish, R.L. Robinson, J. Chem. Eng. Data 34 (1989) 397–398.
[111] S.P. Dastur, Diss. Northwestern Univ., 1964.
[112] V.S. Mehra, G. Thodos, J. Chem. Eng. Data 10 (1965) 211–214.
[113] W.B. Kay, Ind. Eng. Chem. 30 (1938) 459–465.
[114] A.B.J. Rodrigues, D.S. McCaffrey Jr., J.P. Kohn, J. Chem. Eng. Data 13 (1968) 164–168.
[115] W.-L. Weng, M.-J. Lee, J. Chem. Eng. Data 37 (1992) 213–215.
[116] Y. Kobatake, J.H. Hildebrand, J. Phys. Chem. 65 (1961) 331–335.
[117] F.H. Fallaha, Thesis, University of Birmingham, 1974.
[118] H.H. Reamer, B.H. Sage, J. Chem. Eng. Data 7 (1962) 161–168.
[119] B.A. Bufkin, R.L. Robinson, S.S. Estrera, K.D. Luks, J. Chem. Eng. Data 31 (1986) 421–423.
[120] H. Gardeler, K. Fischer, J. Gmehling, Ind. Eng. Chem. Res. 41 (2002) 1051–1056.
[121] S.S. Estera, M.M. Arbuckle, K.D. Luks, Fluid Phase Equilib. 35 (1987) 297–307.
[122] K.A.M. Gasem, R.L. Robinson Jr., J. Chem. Eng. Data 30 (1985) 53–56.
[123] K.H. Lee, J.P. Kohn, J. Chem. Eng. Data 14 (1969) 292–295.
[124] M. Meskel-Lesavre, D. Richon, H. Renon, Ind. Eng. Chem. Fundam. 20 (1981) 284–289.

[125] D. Legret, D. Richon, H. Renon, Ind. Eng. Chem. Fundam. 19 (1980) 122–126.
[126] K.A. Gasem, B.A. Bufkin, A.M. Raff, R.L. Robinson, J. Chem. Eng. Data 34 (1989) 187–191.
[127] C.J. Peters, J.L. De Roo, R.N. Lichtenthaler, Fluid Phase Equilib. 34 (1987) 287–308.
[128] A.Q. Clark, K. Stead, J. Chem. Thermodyn. 20 (1988) 413–428.
[129] W.B. Kay, J. Chem. Eng. Data 15 (1970) 46–52.
[130] P. Beranek, I. Wichterle, Fluid Phase Equilib. 6 (1981) 279–282.
[131] H. Hipkin, AIChE J. 12 (1966) 484–487.
[132] J. Vejrosta, I. Wichterle, Collect. Czech. Chem. Commun. 39 (1974) 1246–1248.
[133] B.H. Sage, W.N. Lacey, Ind. Eng. Chem. 32 (1940) 992–996.
[134] W.E. Vaughan, F.C. Collins, Ind. Eng. Chem. 34 (1942) 885–890.
[135] K. Ishida, K. Noda, K. Hirako, Asahi Garasu Kogyo Gijutsu Shoreikai Kenkyu Hokoku 26 (1975) 355–360.
[136] W.B. Kay, J. Chem. Eng. Data 16 (1971) 137–140.
[137] S.W. Chun, W.B. Kay, J.C. Rainwater, J. Chem. Eng. Data 38 (1993) 494–501.
[138] J.L. Guillevic, D. Richon, H. Renon, Ind. Eng. Chem. Fundam. 22 (1983) 495–499.
[139] W.B. Kay, J. Genco, D.A. Fichtner, J. Chem. Eng. Data 19 (1974) 275–280.
[140] D.W. Jennings, R.C. Schucker, J. Chem. Eng. Data 41 (1996) 831–838.
[141] H.H. Reamer, B.H. Sage, J. Chem. Eng. Data 11 (1966) 17–24.
[142] J. Gregorowicz, T.W. de Loos, J. de Swaan Arons, J. Chem. Eng. Data 37 (1992) 356–358.
[143] J.A. Martinez-Ortiz, D.B. Manley, J. Chem. Eng. Data 23 (1978) 165–167.
[144] K. Yokoyama, S. Ohe, Ishikawajima-Harima Giho 11 (1971) 5–11.
[145] M. Hirata, S. Suda, Bull. Jpn. Petrol. Inst. 10 (1968) 20–27.
[146] G. Calingaert, L.B. Hitchcock, J. Am. Chem. Soc. 49 (1927) 750–765.
[147] W.B. Kay, R.L. Hoffman, O. Davies, J. Chem. Eng. Data 20 (1975) 333–338.
[148] A. Hoepfner, U.T. Kreibich, K. Schaefer, Ber. Bunsenges. Phys. Chem. 74 (1970) 1016–1020.
[149] L.W. Cummings, Sci. Thesis, Mass. Inst. Techn., 1933.
[150] W.B. Kay, Ind. Eng. Chem. 33 (1941) 590–594.
[151] H.H. Reamer, B.H. Sage, J. Chem. Eng. Data 9 (1964) 24–28.
[152] S. Chen, B.I. Zwolinski, J. Chem. Soc., Faraday Trans. II 70 (1974) 1133–1142.
[153] F.G. Tenn, R.W. Missen, Can. J. Chem. Eng. 41 (1963) 12–14.
[154] P. Rice, A. El-Nikheli, Fluid Phase Equilib. 107 (1995) 257–267.
[155] D.L. Katz, G.G. Brown, Ind. Eng. Chem. 25 (1933) 1373–1384.
[156] W.T. Cummings, F.W. Stones, M.A. Volante, Ind. Eng. Chem. 25 (1933) 728–732.
[157] P.L. Chueh, J.M. Prausnitz, in: D. Behrens, R. Eckermann (Eds.), Vapor–Liquid Equilibria for Mixtures of Low Boiling Substances, Chemistry Data Series, VI, DECHEMA, 1982, p. 721.
[158] A.V. Kozhenkov, V.P. Kononov, Yu.I. Malenko, Zh. Prikl. Khim. (Leningrad) 54 (1981) 973–988.
[159] C.L. Ho, R.R. Davison, J. Chem. Eng. Data 24 (1979) 293–296.
[160] H.A. Beatty, G. Calingaert, Ind. Eng. Chem. 26 (1934) 504–508.
[161] C.P. Smyth, E.W. Engel, J. Am. Chem. Soc. 51 (1929) 2646–2660.
[162] V. Zharov, T. Vitman, H. Viit, L. Kudryavtseva, Eesti NSV Tead Akad. Toim. Keem. Geol. 20 (1971) 206–209.
[163] E.H. Leslie, A.R. Carr, Ind. Eng. Chem. 17 (1925) 810–817.
[164] J. Zielkiewicz, J. Chem. Thermodyn. 23 (1991) 605–612.
[165] D.S. Jan, H.Y. Shiau, F.N. Tsai, J. Chem. Eng. Data 39 (1994) 438–440.
[166] H. Kirss, L.S. Kudryavtseva, O. Eisen, Eesti NSV Tead Akad. Toim. Keem. Geol. 24 (1975) 15–22.
[167] S. Weiguo, A.X. Qin, P.J. McElroy, A.G. Williamson, J. Chem. Thermodyn. 22 (1990) 905–914.
[168] K.N. Marsh, J.B. Ott, M.J. Costigan, J. Chem. Thermodyn. 12 (1980) 343–348.
[169] S.K. Ogorodnikov, V.B. Kogan, A.I. Morozova, Zh. Prikl. Khim. 35 (1962) 685–687.
[170] K.N. Marsh, J.B. Ott, A.E. Richards, J. Chem. Thermodyn. 12 (1980) 897–902.
[171] J.B. Ott, K.N. Marsh, R.H. Stokes, J. Chem. Thermodyn. 13 (1981) 371–376.
[172] M.L. McGlashan, A.G. Williamson, Trans. Faraday Soc. 57 (1961) 588–600.
[173] J.H. Hildebrand, J.W. Sweny, J. Phys. Chem. 43 (1939) 109–117.
[174] J.G. Fernandez-Garcia, C.G.M. Guillemin Boissonnas, Helv. Chim. Acta 51 (1968) 1733–1737.
[175] C. Berro, F. Laichoubi, E. Rauzy, J. Chem. Eng. Data 36 (1991) 474–478.
[176] J.A. Abara, D.W. Jennings, W.B. Kay, A.S. Teja, J. Chem. Eng. Data 33 (1988) 242–247.
[177] E.K. Liu, R.R. Davison, J. Chem. Eng. Data 26 (1981) 85–88.
[178] C. Berro, F. Laichoubi, E. Rauzy, J. Chem. Thermodyn. 26 (1994) 863–869.
[179] L.S. Kudryavtseva, A. Viit, O. Eisen, Eesti NSV Tead. Akad. Toim. Keem. Geol. 20 (1971) 292–296.
[180] J. Wisniak, G. Embon, R. Shafir, H. Segura, R. Reich, J. Chem. Eng. Data 42 (1997) 1191–1194.
[181] L. Sieg, Chem. Ing. Tech. 22 (1950) 322–326.
[182] E.C. Bromiley, D. Quiggle, Ing. Eng. Chem. 25 (1933) 1136–1138.
[183] A. Dejoz, V. Gonzalez-Alfaro, P.J. Miguel, M.I. Vazquez, J. Chem. Eng. Data 41 (1996) 93–96.
[184] C.J. Boukouvalas, K.G. Magoulas, S.K. Stamataki, D.P. Tassios, Ind. Eng. Chem. Res. 36 (1997) 5454–5460.
[185] P.H. Van Konynenburg, R.L. Scott, Philos. Trans. R. Soc. Lond., Ser. A 298 (1980) 495–540.
[186] C.P. Hicks, C.L. Young, Chem. Rev. 75 (1975) 119–175.
[187] E.A. Turek, R.S. Metcalfe, L. Yarborough, R.L. Robinson, SPEJ 24 (3) (1984) 308–324.
[188] K. Anastasiades, S. Stamataki, D. Tassios, Fluid Phase Equilib. 34 (1994) 23–54.
[189] S.K. Stamataki, K.G. Magoulas, C.J. Boukouvalas, D.P. Tassios, Revue de l'institut français du pétrole 53 (1) (1998) 59–69.
[190] S. Stamataki, D.P. Tassios, Revue de l'institut français du pétrole 53 (3) (1998) 367–377.
[191] E. Flöter, Th.W. de Loos, J. de Swaan Arons, Fluid Phase Equilib. 127 (1997) 129–146.
[192] J.F. Arnaud, P. Ungerer, E. Behar, G. Moracchini, J. Sanchez, Fluid Phase Equilib. 124 (1996) 177–207.
[193] C.P. Huang, D.S. Jan, F.N. Tsai, J. Chem. Eng. Jpn. 25 (2) (1992) 182–186.
[194] C.J. Peters, H.J. Van der Kooi, J. de Swaan Arons, J. Chem. Thermodyn. 19 (1987) 395–405.
[195] L. Constantinou, R. Gani, AIChE J. 40 (1994) 1697–1710.
[196] L. Constantinou, R. Gani, J.P. O'Connell, Fluid Phase Equilib. 103 (1995) 11–22.
[197] S.H. Huang, H.M. Lin, K.C. Chao, J. Chem. Eng. Data 33 (1988) 143–145.
[198] F.N. Tsai, S.H. Huang, H.M. Lin, K.C. Chao, J. Chem. Eng. Data 32 (1987) 467–469.
[199] A.J. Ashworth, J. Chem. Soc., Faraday Trans. 1: Phys. Chem. Condensed Phases 69 (2) (1973) 459–466.
[200] J.L. Daridon, P. Xans, F. Montel, Fluid Phase Equilib. 117 (1996) 241–248.